



Article

Critical Analysis of the Materials Used by the Venetian Artist Guido Cadorin (1892–1976) during the Mid-20th Century, Using a Multi-Analytical Approach

Erik Guillermo Morales Toledo ¹, Teodora Raicu ¹, Laura Falchi ¹ , Elisabetta Barisoni ², Matteo Piccolo ² and Francesca Caterina Izzo ^{1,*} 

¹ Sciences and Technologies for the Conservation of Cultural Heritage, Department of Environmental Sciences, Informatics and Statistics, Ca' Foscari University of Venice, Via Torino 155/b, 30173 Venice, Italy

² Fondazione Musei Civici, MUVE—Galleria Internazionale d'Arte Moderna di Ca' Pesaro, Santa Croce 2076, 30135 Venice, Italy

* Correspondence: fra.izzo@unive.it

Abstract: The present study sought to expand on and confirm the already available information on the painting materials used by the Venetian artist Guido Cadorin (1892–1976). A multi-analytical approach was employed in the study of six *tempera grassa* easel paintings and one casein tempera on a panel signed by the artist and belonging to the International Gallery of Modern Art Ca' Pesaro in Venice, Italy, which dated from 1921 to 1951. The aim of the research was to identify the painting materials, observe the evolution of the color palette through time and assess the state of conservation. Non-invasive imaging and/or spectroscopic techniques were employed, such as hyperspectral imaging spectroscopy (HSI) and Raman spectroscopy. Microsamples were also collected from the edges and detached areas of the canvases that were studied through three non-destructive techniques, namely optical microscopy (OM), energy dispersive x-ray fluorescence spectrometry (EDXRF) and attenuated total reflection fourier transform infrared spectroscopy (ATR-FTIR), and one destructive technique, namely gas chromatography-mass spectrometry (GC/MS). The results allowed the inference of the color palette used to render the artist's paints, composition of the preparation layer, and characterization of the binding media and varnish layers. Moreover, the state of conservation of the artworks was determined. Thus, the outcome of this research enriches the painter's profile and might aid the International Gallery of Modern Art Ca' Pesaro in Venice, Italy in the planning of future conservation treatments in accordance with the guidelines of good practices in art conservation.

Keywords: cultural heritage; Guido Cadorin; heritage science; modern materials; modern oil painting; hyperspectral imaging spectroscopy; ATR-FTIR; Raman spectroscopy; GC-MS; tempera grassa



Citation: Morales Toledo, E.G.; Raicu, T.; Falchi, L.; Barisoni, E.; Piccolo, M.; Izzo, F.C. Critical Analysis of the Materials Used by the Venetian Artist Guido Cadorin (1892–1976) during the Mid-20th Century, Using a Multi-Analytical Approach. *Heritage* **2023**, *6*, 600–627. <https://doi.org/10.3390/heritage6010032>

Academic Editor: Francesco Paolo Romano

Received: 30 November 2022

Revised: 23 December 2022

Accepted: 23 December 2022

Published: 11 January 2023



Copyright: © 2023 by the authors. Licensee MDPI, Basel, Switzerland. This article is an open access article distributed under the terms and conditions of the Creative Commons Attribution (CC BY) license (<https://creativecommons.org/licenses/by/4.0/>).

1. Introduction

It is known that tempera painting had an important revival between 1800–1950 both in Europe and North America, which might be attributed to the fact that modern easel paintings had the tendency to deteriorate easily [1]. Therefore, many artists started to believe that tempera was “superior” to oil as it seemed to be more durable. This revival was mainly triggered on German lands, as many scholars were discussing and reviewing this painting technique compared with other countries, such as Italy [2,3]. However, tempera was still highly employed in Italy at the end of the 19th century, and especially in the Veneto region as it belonged to the Austrian Empire and, thus, was influenced by Austrian/German artists and scholars who had moved to Venice (such as Benno Geiger). One of the most important Venetian artists who largely used this painting technique was Guido Cadorin (1892–1976). He was one of the most important figures of Italian art of the 20th century distinguishing himself through his originality and contribution to the Italian Liberty movement [4], which was considered the Italian version of Art Nouveau.

Moreover, despite his admiration of the secessionist style and emergence of cubism and futurism, he tried to develop his own style, now known as *Magical Realism* [4]. Regarding his preferred painting technique, he became passionate about tempera at the tender age of 15 when he was the pupil of Cesare Laurenti, a painter who was keen on using *tempera grassa* and had clear connections to Germany since he exhibited his works there. Moreover, on the 29th of August 1934, Guido Cadorin wrote to Mariano Fortuny y Madrazo [5], who was notorious for his tempera recipes through which he produced the *Tempere Fortuny* [6], a letter of appreciation of his painting technique. Therefore, Guido Cadorin was clearly focused on developing his own tempera and searched to expand his horizons by acquiring knowledge from other important artists who used similar techniques [6].

Seven paintings of Guido Cadorin were considered in this study, all being part of the permanent collection of the International Gallery of Modern Art Ca' Pesaro in Venice (Italy), which is affiliated with the Fondazione Musei Civici of Venice (MUVE), namely: *Ritratto di mio padre* (1921–23), *Fanciulla* (1930), *Nudo femminile* (c.1930), *La Navicella di San Pietro* (1942), *Ritratto di Giovanni Giurati Junior* (1942), *Ritratto di Benno Geiger* (1943), and *La tavola* (1951), which are shown in Figure 1. Their state of conservation was generally considered to be optimal, with minor cracks due to aging or micro lacunae and paint detachments. The only painting that exhibited a wider and more problematic network of cracks was *La Tavola*, which might be explained by the thick impasto that it consists of.

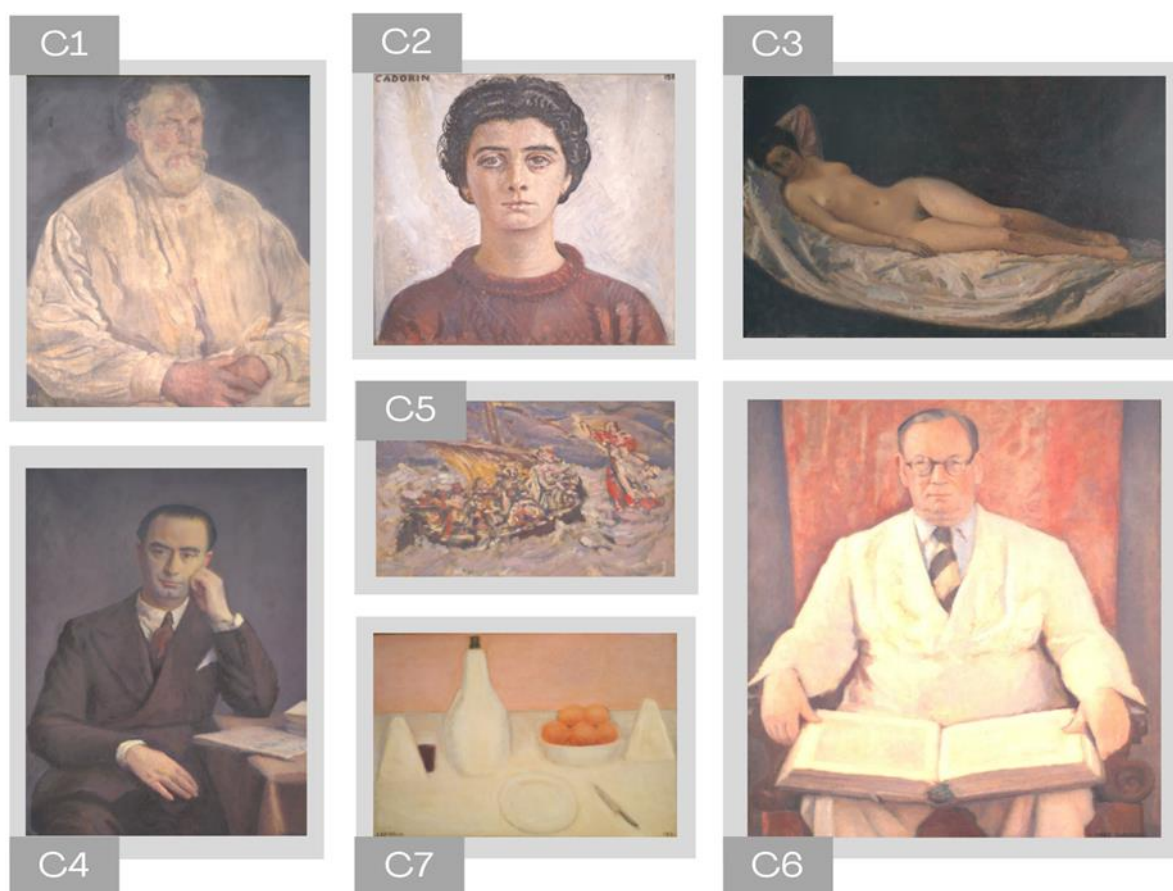


Figure 1. The seven paintings of Guido Cadorin that were analyzed in this study together with their corresponding codes: *Ritratto di mio padre* (1921–23) (C1), *Fanciulla* (1930) (C2), *Nudo femminile* (c.1930) (C3), *Ritratto di Giovanni Giurati Junior* (1942) (C4), *La Navicella di San Pietro* (1942) (C5), *Ritratto di Benno Geiger* (1943) (C6), and *La tavola* (1951) (C7).

According to the literature, only one analytical study has been previously carried out on the artworks of Guido Cadorin, and more specifically on *Ragazza in Verde* (1924) from the Revoltella Museum in Trieste, *Donna nuda* (1920) from the International Gallery of

Modern Art Ca' Pesaro in Venice, and one of the seven aforementioned paintings, namely *Ritratto di Benno Geiger* (C6) [7]. From these works, it was concluded that Cadorin preferred the use of the alleged *tempera grassa*, following closely the recipes of his master Cesare Laurenti. Thus, he mainly painted with a mixture of siccative oils (mostly linseed oil), natural terpenic resins, egg yolk, and animal glue to which he added other materials to change some physical properties of the impasto. Polysaccharides were detected as well, which might have been present due to the addition of flour paste or starch to obtain a stronger impasto. However, despite the lack of gum Arabic in the case of C6, there is a high probability of finding it in the other paintings, since Laurenti's recipes highlight its use in dark colors. The exact purpose of its addition is not entirely understood, but the reconstructions of the recipe by Giovanni Soccol have proved that gum Arabic combined with linseed mucilage can provide an optimal spread of thin layers of paint (*velature*) [7]. Additionally, Cadorin apparently prepared his own paints using recipes and creating them in his workshop in contrast with his master Cesare Laurenti that chose to industrially manufacture them [3].

Therefore, the present study sought to expand the previous findings to better understand Guido Cadorin's technique and analyze its evolution through time. Consequently, the multi-analytical study that was performed on the seven paintings focused on the identification of the painting materials, namely pigments, inorganic additives, binding media, varnishes, and degradation products using both non-invasive (hyperspectral imaging spectroscopy-HSI, raman spectroscopy) and invasive (micro-destructive) techniques (optical microscopy-OM, attenuated total reflection fourier transform infrared spectroscopy-ATR-FTIR, and gas chromatography-mass spectrometry-GC/MS). *Ritratto di Benno Geiger* (C6) was reanalyzed to broaden the earlier results [7] using two additional analytical techniques, namely hyperspectral imaging spectroscopy (HSI) and Raman spectroscopy. Furthermore, it should be noted that the same binding media as in the formerly examined paintings were expected to be found in the case of the analyzed artworks. The only exception would be *Fanciulla* (C1) as it was depicted on a lime-based support, in the case of which Cadorin generally opted for the use of casein tempera [7].

This research helped understand Guido Cadorin's manner of creating the *tempera grassa* throughout time, since the artist left no recipes behind. However, the comparisons with the previous findings from his paintings and those of Cesare Laurenti, Mariano Fortuny, and Giorgio De Chirico aided in narrowing the research and placing his artworks in context. Still, Guido Cadorin did clearly employ complex paint systems and used a variety of different materials that might burden the process of conservation. Therefore, the knowledge of this Venetian artist's painting materials and their degradation products allow for subsequent planning of preventive and even curative conservation treatments.

2. Materials and Methods

2.1. Non-Invasive Analytical Techniques

2.1.1. Macro-Observation

A careful visual and direct inspection of the paintings, also called condition assessment, was conducted as a first step of the analysis together with the conservator of the gallery, Dr. Matteo Piccolo.

2.1.2. Hyperspectral Imaging Spectroscopy (HSI)

The hyperspectral analysis was conducted using the novel hyperspectral camera Specim IQ (Oulu, Finland), with the following specifications: Model VNIR 400–1000 nm (CMOS), 4.3 " touch screen with 5 Mpx camera, interface Specim IQ Studio, battery 5200 mAh Li-Ion (Type 26650) with an operational time of approx. 100 measurements with one SD external card, dimensions 207 × 91 × 74 mm (depth with lens 125.5 mm) weighing approx. 1.3 kg, wavelength 400–1000 nm with a 7 nm resolution, spatial sampling of 512 × 512 pixels, and 204 spectral bands [8]. Thus, the hyperspectral camera acquires a dataset called a data-cube that offers a resolved reflectance spectrum for each of the pixels

which compose the image [9]. Consequently, assumptions could be made regarding the use of particular pigments in multiple regions since reflectance spectra were obtained that ranged from 397 to 1004 nm [10]. The images were taken in outdoor lighting conditions. These conditions were characterized by the camera through the measurement of the white reference (99% BaSO₄-Specim) that was included in all photos and the subsequent selection of 100 random spectra from the white reference that were averaged and employed for the normalization of data reflectance. All these processes were automatically performed by the device. However, notably, an increase in noise and reflectance was observed in the 900–1004 nm range. This might have been triggered by the absorption band of atmospheric water (H₂O), which is found in the 925–970 nm range and causes an increase in the observed reflectance, in accordance with the information provided by the manufacturer [8].

Specim IQ studio software was used to further process the data since it enabled the construction of precision masks to highlight areas with comparable spectral properties based on the variance of the spectra gathered, and it averaged all the spectra into one. The creation of maps of pixels was automatically made by the software using the spectral angle mapper (SAM) algorithm, which calculates the spectral similarity between two or more spectra by measuring the angle between them [11]. In accordance with [12,13], to generate the mapping procedure, a wide thresholding (SAM Tolerance) was picked from the maximum angle (expressed in radians) area by using the SAM mask tool. Therefore, the selection was manually made from 0.95 to 1.0 and changed until the best optimized maps were obtained.

2.1.3. Raman Spectroscopy

For the Raman analysis, a Bravo Bruker Optics portable spectrophotometer was used. This instrument was developed for easy identification of chemical compounds and includes built-in wavelength calibration for precision [14]. It is a highly automated handheld device with a rectangular shape that only weighs about 1.5 kg [15]. It has a duo-laser excitation system with two near-infrared lasers (785 and 853 nm in wavelength) that operate in a sequentially shifted mode to suppress fluorescence and can be controlled using a touchscreen display. The automatic mode was used for all the measurements. It has a fixed laser power of about 100 mW and a spectral range of 300–3200 cm⁻¹, with a spectral resolution of 10 cm⁻¹ and an output power of <100 mW [16]. Each measurement generally took around 2 min.

2.2. Invasive and/or Micro-Destructive Analytical Techniques

2.2.1. Micro-Sampling and Optical Microscopy (OM)

The removal of micro-samples (less than 0.1 mg in weight) from the seven works-of-art was planned and conducted with the assistance of the conservator Dr. Matteo Piccolo, after having received prior permission from the superintendence of the city of Venice and its municipality. The samples were collected from the regions of the canvases that presented detachments or from the marginal parts covered by the frame and, thus, their removal would not be visually noticed. In the case of the latter, the micro-samples were collected after their detachment using a scalpel.

Optical microscopy analysis was performed for observing the samples (see Appendix A, Table A1). A bench microscope ZEISS SteREO Discovery.V8 (Carl Zeiss Microscopy GmbH) was used, which is a modular microscope equipped with a manual 8:1 zoom, a manual or motorized focus and two ZEISS Achromat S Objectives of 0.63× and 1.5×. The digital camera used by the microscope is a ZEISS AxioCam 208 color full 4K resolution at 30 fps.

2.2.2. Energy Dispersive X-ray Fluorescence Spectrometry (EDXRF)

Energy dispersive X-ray fluorescence spectrometry (EDXRF) was used for the preliminary identification of inorganic pigments and additives. It was conducted on three samples extracted from the C4 (one sample of white paint – C₄₋₁₂) and C7 (one sample

of white paint – C₇₋₂₀ –, and one of red paint – C₇₋₂₂ –; both collected from the back of the artwork and supposed to match the paints on the front side). CRONO non-contact micro-XRF scanning spectrometer (Bruker Optik GmbH) was employed. This instrument is generally used for rendering a 2D mapping of the examined painting. However, in this study, it was converted into a portable XRF device that allowed the non-contact punctual analysis of samples through the installation of the measurement head on a tripod. The spectrometer was set to a voltage of 40 kV, a current of 2 μ A and a timeframe of 40 s. To properly interpret the obtained data, the X-ray transition application (RaySpec X-ray Spectroscopy) was used, which is equipped with reference values extracted from the NIST Standard Reference Database 128 created by Deslattes et. al. [17], which comprises the X-ray transition energies for all elements from neon (Ne) to fermium (Fm) [18].

2.2.3. Attenuated Total Reflection Fourier Transform Infrared Spectroscopy (ATR-FTIR)

In the present research, a Bruker ALPHA II Fourier Transform IR Spectrometer was also used in ATR-FTIR mode. ATR-FTIR spectra were recorded in the spectral range from 4000 to 400 cm^{-1} , using a synthetic diamond crystal over glass for the compression of the samples. The background was measured with 48 scans before each analysis, while samples were registered using 128 scans with a 4 cm^{-1} resolution. Data acquisition was managed through OPUS software (Version 8.2.28). The spectra were further elaborated using Origin 2019b (9.65).

2.2.4. Gas Chromatography-Mass Spectrometry (GC-MS)

Gas chromatography-mass spectrometry (GC-MS) was performed on a part of the micro-samples taken from detached areas, borders and/or the backside of the support of the artworks. It was mainly applied to characterize the binding media used by the artist and other organic compounds, eventually degradation products. A Trace GC 1300 system equipped with an ISQ 7000 MS detector with a quadrupole analyzer was used (ThermoFisher Scientific, Waltham, MI, USA). Then, 1 μ L of each derivatized sample was injected by a AS1310 autosampler (ThermoFisher Scientific, Waltham, MI, USA). Helium was employed as the carrier gas (flow rate 1 mL/min), and the GC separation was performed on a chemically attached fused silica capillary DB-5MS Column (30 m length, 0.25 mm, 0.25 μm —5% phenyl methyl polysiloxane). The MS interface and inlet temperature were both set to 280 °C. The MS source temperature was set to 300 °C and transfer line to 280 °C. The MS was conducted at 1.9 scans per second in full scan mode (m/z 40–650). There was a 70 eV electron ionization energy. The compounds were qualitatively identified by comparing their mass spectra to those from the libraries (such as NIST and MS Search 1.7) and ad hoc databases created by the authors. The Chromeleon 7 software was used for the data acquisition and processing. The microsamples (approximately 0.1 mg) were accurately weighted and placed into micro vials, then transesterified using (trifluoromethylphenyl)trimethylammonium hydroxide (5% in methanol); the reaction taking place overnight in accordance with the methodology presented in [19,20]. Using nonadecanoic acid as the internal standard (10 μ L of 1 mM nonadecanoic acid in a methanol solution in each of the micro vials), quantitative analysis could also be performed.

The following fatty acid molar ratios were determined to observe the degree to which the lipidic binding media had oxidized: P/S (palmitic-to-stearic acid ratio) that is frequently used to determine the kind of drying/non-drying oils which have been employed; A/P (azelaic acid-to-palmitic acid ratio) that is used to distinguish drying oils from egg lipids; D/P (the total sum of dicarboxylic acids-to-palmitic acid ratio) that has a similar purpose to A/P; Σ D (the total sum of dicarboxylic acids) that is also used to determine the type of lipid binder; O/S (oleic acid-to-stearic acid ratio) that may indicate the maturity of oils (i.e., the quantity of unsaturated fatty acids still present); and A/Sub (azelaic acid-to-suberic acid ratio) [21–25].

3. Results and Discussion

3.1. Preparatory Layer

The preparatory layers of all seven artworks consisted of gypsum, together with barite, calcite, barium white/lithopone and/or lead white, according to Table 3 and Figure 2. Gypsum was mainly observed in the Raman spectra through its characteristic signal at ca. 1008 cm^{-1} that is related to the ν_1 symmetric stretching vibration mode of the SO_4^{2-} ion [26]. The presence of barium white and/or lithopone was generally observed in the Raman spectra as its specific bands at ca. 450 and 988 cm^{-1} were always present. Thus, it might have been purposefully used as a filler due to properties such as its fine nature, ease of dispersibility, and low-degree of replacing the binder [27]. It should be mentioned that titanium white, in the anatase form, might have been produced through the co-precipitation with barium white and gypsum [28], which could also explain the presence of those two compounds in all spectra.

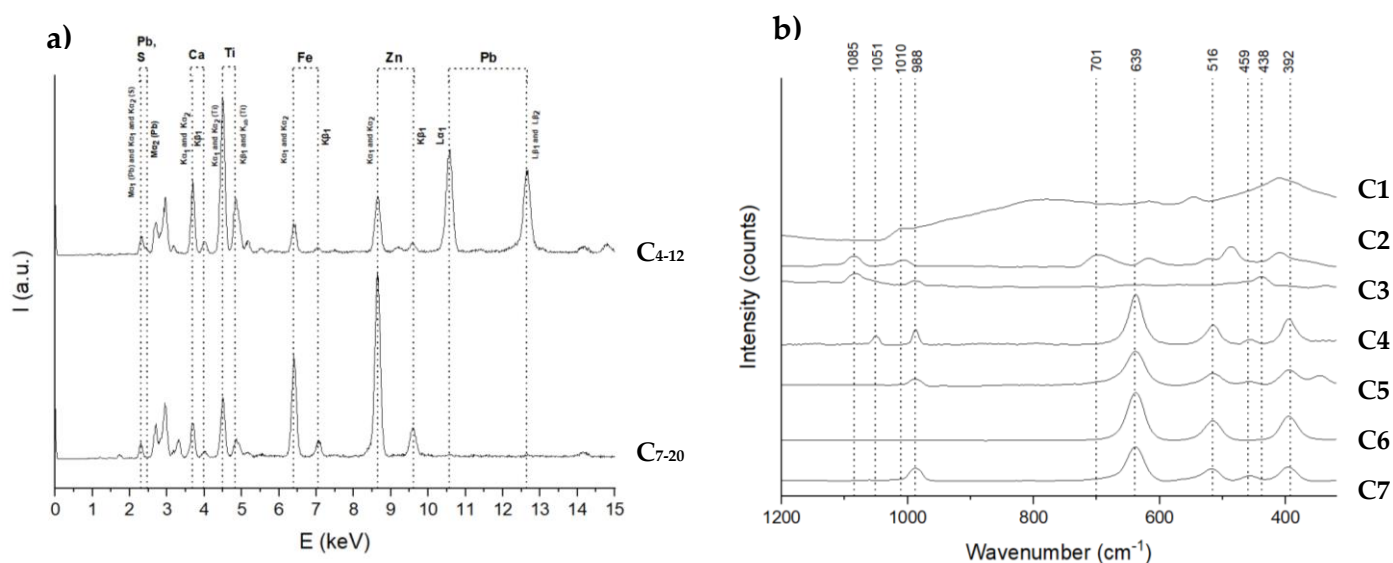


Figure 2. The white paint XRF (a) and Raman spectra (b) that also highlight the components of the preparatory layers.

Moreover, the existence of calcite was firstly observed through Raman as the spectra included its specific band at ca. 1085 cm^{-1} , typical for the symmetric stretching vibration of the CO_3^{2-} ion [29] that was additionally confirmed by XRF as calcium's (Ca) emission lines were identified at around 3.69 keV ($\text{K}\alpha_1$ and $\text{K}\alpha_2$) and 4.01 keV ($\text{K}\beta_1$ and $\text{K}\beta_2$). The predominance of gypsum, barite/lithopone, and calcite could be further confirmed by ATR-FTIR, as emphasized in Table 3. Lead white ($2\text{PbCO}_3 \times \text{Pb}(\text{OH})_2$) was observed only in C4 according to the Raman signal detected at 1051 cm^{-1} [30], whose existence could be explained by the use of a commercially primed canvas that consisted of cerussite. This result was also highlighted by XRF, as the following emission lines corresponding to Pb were identified, namely at 10.45 keV ($\text{L}\alpha_1$ and $\text{L}\alpha_2$), 12.61 keV ($\text{L}\beta_1$ and $\text{L}\beta_2$), and 2.34 and 2.44 keV ($\text{M}\alpha_1$ and $\text{M}\alpha_2$). However, the specific emission line of sulfur (S) was also identified at approximately 2.30 keV ($\text{K}\alpha_2$), which might be overlapped with the aforementioned 2.34 keV signal of Pb ($\text{M}\alpha_1$) in the case of C4. In spite of this, its presence might strengthen the use of lithopone/barium white and/or gypsum.

3.2. Paint Layers

3.2.1. White Paints

White paint (Figure 2) was difficult to observe in the case of C1, as the only white material that was identified using Raman spectroscopy was gypsum at 1008 cm^{-1} (Figure 2b), which most probably belonged to the preparatory layer. This could be explained by the

presence of a thick layer of varnish (see Appendix A, Table A1) that might have enhanced the background fluorescence emission, which rendered the detection of other painting materials difficult [31]. Still, zinc carboxylates were observed in C1 using ATR-FTIR (see Table 3), which might suggest the use of zinc white/lithopone as a white paint.

C2 was another particular case since it was depicted on a lime-based support. Therefore, the Raman peak found at 1085 cm^{-1} (Figure 2b), which was attributed to calcite, might also emphasize the preference of the artist for the use of CaCO_3 both for preparing the support and rendering the white paint. The only painting in which the presence of zinc white could be observed was C3, according to the Raman signal detected at approximately 438 cm^{-1} meaning retained $^{-1}$ [30]. In spite of this, zinc (Zn) was also identified through XRF (Figure 2a) in C4 and C7 according to the signals at around 8.61 keV ($\text{K}\alpha_1$ and $\text{K}\alpha_2$) and 9.6 keV ($\text{K}\beta_1$ and $\text{K}\beta_2$), which could be attributed to zinc white (ZnO). Lithopone ($\text{ZnS} + \text{BaSO}_4$) is unlikely to have been present in the analyzed samples (both in C4 and C7), since the K emission lines of barium (Ba) that should have been visible at ca. 32 keV were nonexistent. However, barite/lithopone was observed with the use of Raman as shown in Table 3, most probably because the paint layers had been analyzed in their entirety in this case, whereas in XRF only the samples that presented only the pigment layer, namely the superficial one, had been used. Therefore, this aspect might highlight its use as an extender in the preparatory layers.

Titanium white (TiO_2) in the anatase form was identified in the artworks dating from 1940 onward (C4, C5, C6, and C7), according to the three typical Raman peaks [30] observed at 638 , 516 , and 394 cm^{-1} (Figure 2b). The XRF spectra additionally confirmed the presence of titanium (Ti) according to the signals detected at around 4.50 keV ($\text{K}\alpha_1$ and $\text{K}\alpha_2$) and 4.95 keV ($\text{K}\beta_1$ and K_{ab}) (Figure 2a). Thus, it might be hypothesized that Guido Cadorin started to use paint tubes in the case of titanium white from 1940 onward since zinc white might have been present its paint formulation together with calcite (CaCO_3), probably even with metal stearates (such as aluminum stearates), which were typically added in tubes to prevent oil separation [32] and in time might enhance the formation of metal soaps [33–35].

3.2.2. Black and Brown Paints

On the other hand, for rendering the black color, the artist seems to have used carbon-black pigments in all the analyzed artworks, since their specific Raman bands, namely D (that represents the defects in the lattice structure of the amorphous carbon) and G (that stands for *graphitic*, which is connected to the graphitized structure of carbon characterized by sp^2 hybridized C-atoms), were identified at ca. 1300 cm^{-1} (D-band) and 1600 cm^{-1} (G-band), respectively [27,30,36]. Moreover, the use of these pigments was also emphasized by ATR-FTIR (see Table 3), the spectrum being compared to the reference provided by the Institute of Chemistry of the University of Tartu, Estonia [37]. Despite this, the exact type of employed carbon-black pigments could not be distinguished since their characteristic bands are very similar. However, other modern painters such as Giorgio De Chirico used both ivory and vine black paints [38], thus Guido Cadorin might have also mixed these two pigments.

Brown paint was detected only in C4 (Figure 3a) through the presence of a broad band at 648 cm^{-1} , which suggested the use of burnt umber [31,32]. This pigment was identified together with vermilion, and thus it might have been used for darkening the hue of the latter.

3.2.3. Red Paints

Similar to white, red paint differed according to the period. Initially, red ochre in the form of hematite (Fe_2O_3) was used, thus before and around 1930 (C1, C2, and C3). The presence of this pigment was hypothesized at first due to its specific inflection points and slopes found in the HSI spectra [39]. The maximum inflection point was identified at ca. $575\text{--}590\text{ nm}$, and the distinctive positive slope in the region above 600 nm consisted of a less pronounced inflection point at ca. 700 nm (see Appendix B, Figure A1). However, this

hypothesis could be confirmed by the Raman spectra (Figure 3a). The bands located at ca. 410 and 617 cm^{-1} corresponded to the Fe-O symmetric bending vibrations [40,41].

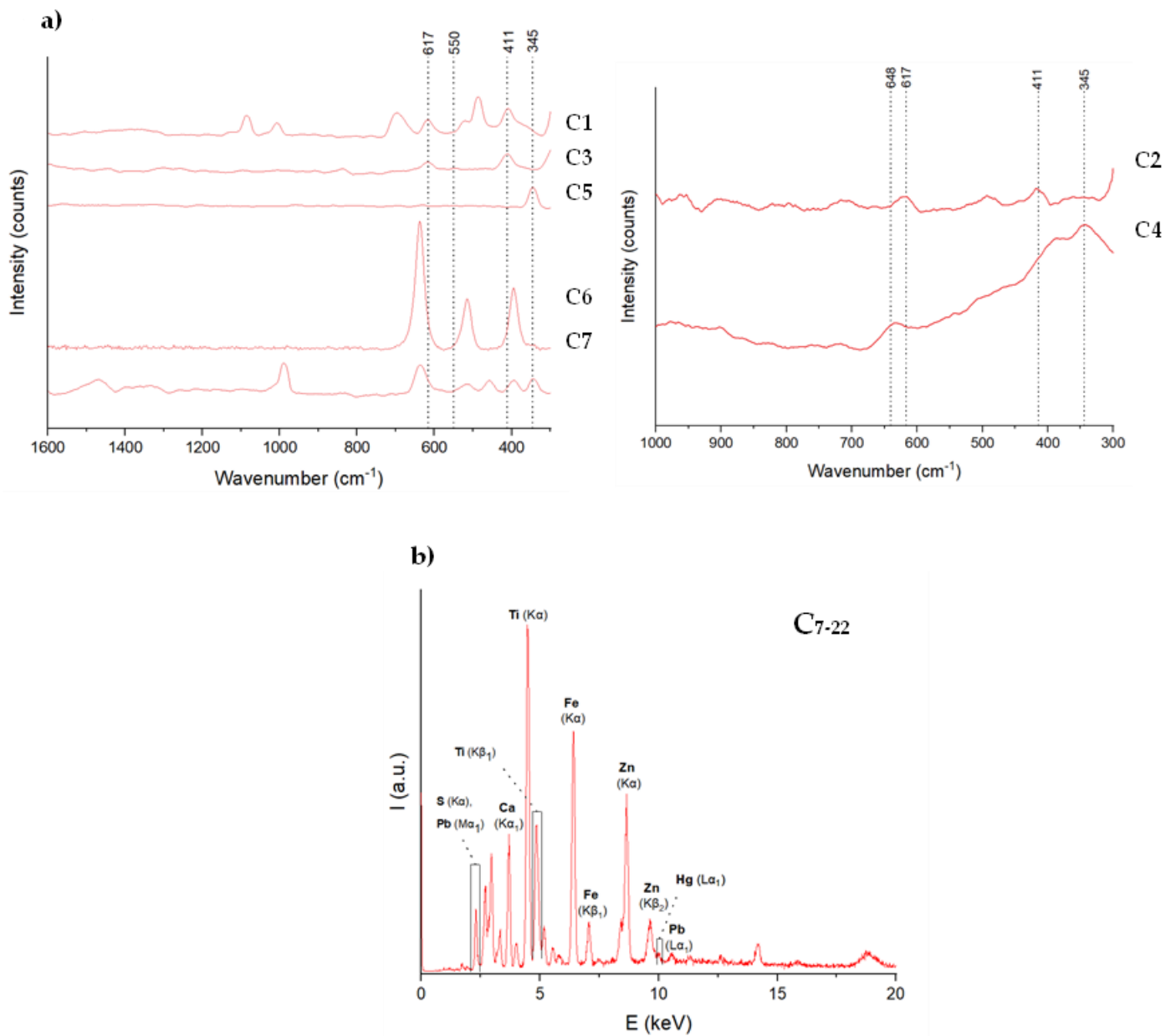


Figure 3. The Raman spectra (a) that emphasize the use of hematite in (C1, C2, and C3) and cinnabar/vermilion (C4, C5, C6, and C7). Moreover, the presence of burnt umber is also observable in C4. The XRF spectrum of the C₇₋₂₂ sample (b) that indicates the use of cinnabar/vermilion and red lead, which probably acted as an adulterant.

After 1940 (C4, C5, C6, and C7), vermilion (HgS) seems to have replaced the former, as the specific peak at ca. 344 cm^{-1} started to emerge within the Raman spectra. Moreover, the XRF spectrum of the C₇₋₂₂ sample (Figure 3b) confirms the presence of mercury sulfide (HgS), according to the observed specific emission lines of mercury (Hg), namely at around 9.89 keV ($L\alpha_1$ and $L\alpha_2$). Additionally, the signal observed at around 2.30 keV might emphasize its use due to the seemingly concomitant presence of Hg ($M\alpha_2$) and sulfur—S ($K\alpha_1$ and $K\alpha_2$). Nonetheless, low intensity signals specific for lead (Pb) were also detected in C7, namely at around 10.45 keV ($L\alpha_1$ and $L\alpha_2$), which could highlight the use of a small amount of red lead (Pb_3O_4). Therefore, the emission line around 2.30 keV might

also be attributed to Pb ($M\alpha_1$). Furthermore, the Raman spectrum of the red paint in C7 has revealed a weak signal at 550 cm^{-1} , which might be assigned to the stretching vibrations of $\nu(\text{Pb-O})$ [42]. The addition of red lead was routinely performed since the Middle Ages as the cost of cinnabar red was higher than that of minimum [43], thus the pigment acted as an adulterant. Moreover, the Bologna manuscript (dated around 1930) firstly mentioned the use of lead compounds as siccative for oils [44], which continued to be employed throughout the ages till they were banned from use in 1961 in Italy [45] and 1987 in the UK [46]. It should also be mentioned that the quantity of lead drier that was generally needed was of 1–2% per weight of oil, this being enough to reduce the drying time [46], which might explain the weak signals that were observed in the XRF spectrum corresponding to the red paint of C7. Therefore, as Izzo et al. [7] suggested, the technique of Guido Cadorin was characterized by the use of traditional painting materials, and thus he might have added the adulterant/siccative himself.

3.2.4. Blue and Purple Paints

The HSI reflectance spectra (see Appendix B, Figure A2) seemed to underline the presence of ultramarine blue in C3, C4, C5, and C6. The intense absorption band whose peak was observed at 600 nm could be assigned to this pigment, as it might have corresponded to the S_3^- anion [47]. This was also accompanied by a weaker band at ca. 480 nm that could be attributed to the S_2^- anion. However, pigments such as cobalt blue and phthalocyanine blue are characterized by the same bands [48], and thus the identification of this pigment using HSI is highly hypothetical. Still, the use of ultramarine blue was confirmed by its specific absorption band at ca. 547 cm^{-1} (observed in all paintings except for C2 and C3) that was identified in the Raman spectra (Figure 4a). Furthermore, this was further supported by ATR-FTIR (see Table 3), the spectrum being compared to the reference provided by the Institute of Chemistry, University of Tartu, Estonia [49]. However, it should be noted that the pigment was most probably not natural since it was rather expensive, and artists might have preferred to use its synthetic version. This was indicated by the lack of the absorption band at ca. 2340 cm^{-1} by ATR-FTIR, which is specific to this natural blue pigment as it represents the asymmetric stretching of CO_2 molecules that are captured within the structure of the rock of lapis lazuli during its geological formation [50].

It was observed that Guido Cadorin tended to create the purple color by mixing red and blue paints. According to the Raman spectrum registered in the case of C2 (Figure 4b), red ochre/hematite (Fe_2O_3) was found in the purple color (the two specific bands at 410 and 618 cm^{-1} [40]), but no characteristic peaks for ultramarine blue or other blue pigments were distinguished.

3.2.5. Yellow Paints

Yellow paints were seemingly employed by the artist only in the case of C5 and C7. The signals at 702 and 1314 cm^{-1} found in the Raman spectrum recorded from C5 could have been attributed to the presence of a warm ochre pigment, most probably a golden-ochre that is also referred to as *ocra d'oro d'Italia* [51]. However, the two bands that were encountered in the Raman spectrum from C5 were non-distinguishable for C7, but there was a weak signal at 842 cm^{-1} that might correspond to the same pigment, namely Italiangold ochre. The presence of this pigment seems to be further confirmed by the ATR-FTIR spectrum (shown in Figure 5a) as the peaks that were identified at ca. 465 and 407 cm^{-1} could be attributed to the Fe–O vibrations specific to Italian gold ochre [52].

3.2.6. Green Paints

Green paints could be observed exclusively in the case of C5 after the OM analysis of the C_{5-16} sample (shown in Appendix A, Table A1) was conducted. Accordingly, the green pigment was intense, but it was present strictly underneath the blue paint and, thus, it was invisible to the unaided eye. Consequently, the Raman spectrum of the blue paint consisted of a peak at ca. 879 cm^{-1} (Figure 4a) that could be assigned to the symmetric stretching

of Cr–O in the hydrated Chromium green oxide ($\text{Cr}_2\text{O}_3 \cdot 2\text{H}_2\text{O}$) tetrahedron geometry [53]. However, the use of this pigment was confirmed by the ATR-FTIR spectrum (shown in Figure 5b) due to the observed signals at 632, 538, 523, 459, and 435 cm^{-1} that could be attributed to the vibration of the oxide bond [54,55].

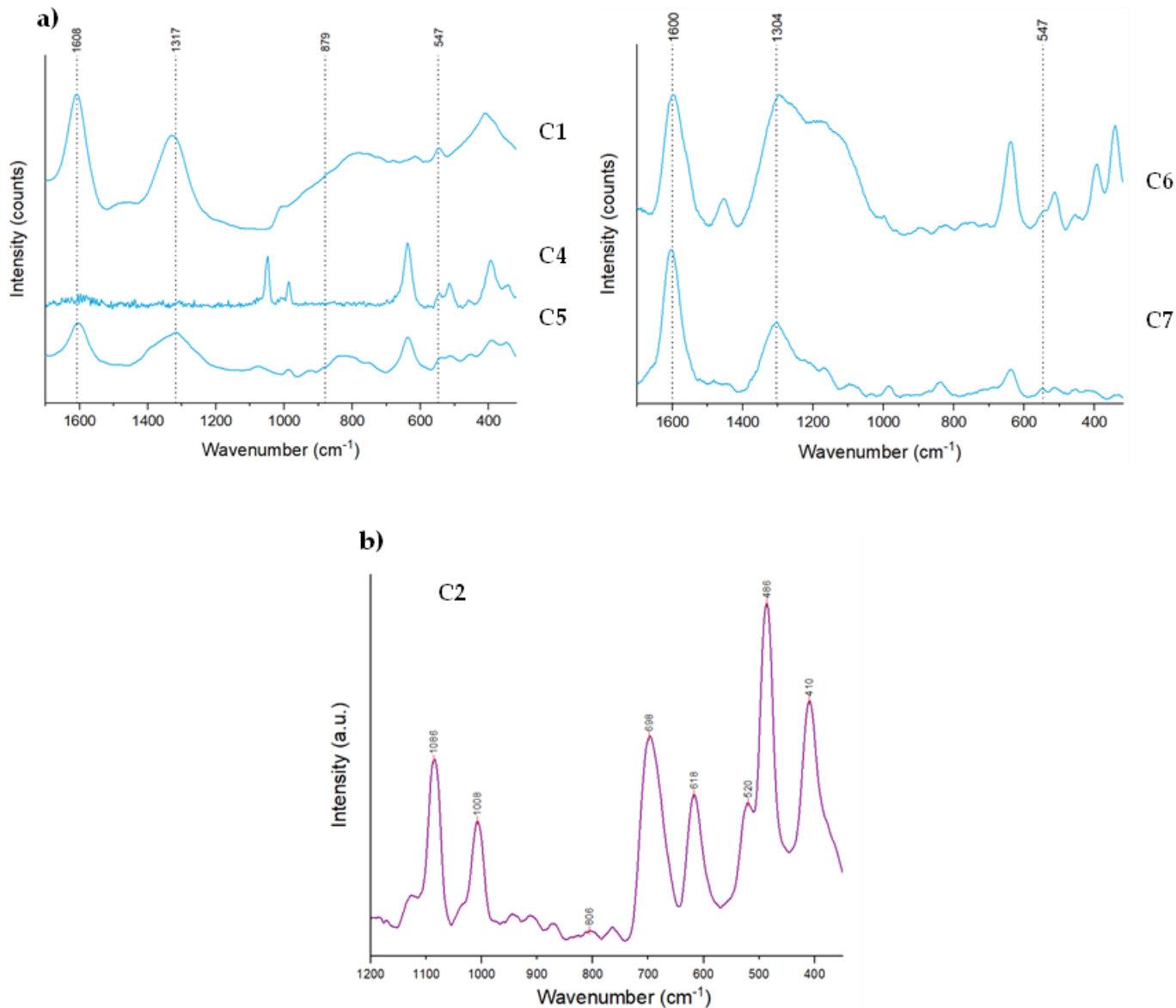


Figure 4. The blue Raman spectra (a) that emphasize the use of ultramarine blue (C1, C5, C6, and C7). Moreover, the presence of the D and G bands corresponding to carbon-black pigments are easily observable in C1, C5, C6, and C7 (a). The Raman spectrum of the purple paint of C2 (b) that highlights the use of hematite through the 618 and 410 cm^{-1} peaks.

3.3. Binding Media and Their Degradation Products

The characterization of the binding media was mainly accomplished by ATR-FTIR and GC-MS. The first technique allowed the prior identification of the type of binding media, which resulted in a mixture of lipid- and protein-based materials. The use of an oil-binder was suggested by the C–H stretching bands around 2800–3000 cm^{-1} and the C=O stretch at ca. 1740 cm^{-1} [56] (Figure 6). The IR peaks that marked the existence of proteinaceous materials were also identified, namely at ca. 1663 cm^{-1} (Amide I) and 1255 cm^{-1} (Amide III) [57], which might suggest the use of egg yolk and/or animal glue (Figure 6a,c). The only exception was C2 (Figure 6b), which presented a lime-based binder,

which seemed to have been predominant due to the multitude of wavenumbers that could be attributed to calcite ($1407, 871, 713 \text{ cm}^{-1}$) [58]. In spite of this, it is worth noting that the proteinaceous materials were also present in this case, which could be assigned to casein. The aggregate that was used for rendering the lime-based support was silicatic, according to the strong signal that was observed at 486 cm^{-1} (D_0 band) which corresponds to the symmetric stretch of three oxygen atoms that are attached to the silicon atom [59]. Furthermore, the shoulder band found at 701 cm^{-1} (Figure 6b), which is due to the $\nu_4 \text{ CO}_3^{2-}$ vibration, could be attributed to the presence of aragonite (one of the mineralogical forms of calcium carbonate; the other form is calcite) [60]. However, further research is recommended to fully demonstrate its existence using scanning electron microscopy (SEM) and x-ray diffraction (XRD), in accordance with [60].

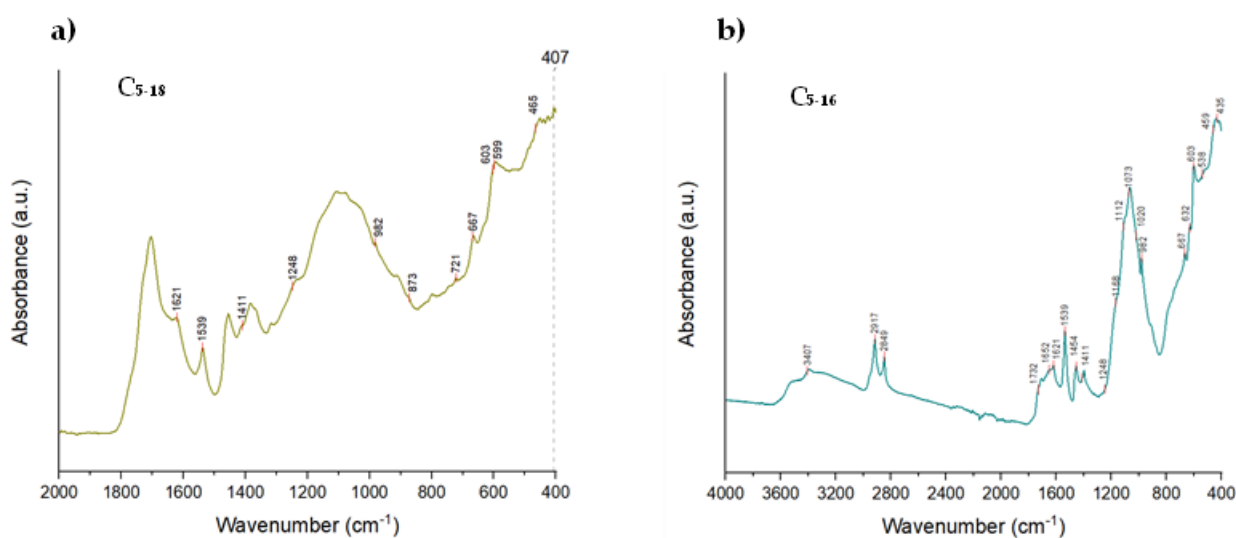


Figure 5. The ATR-FTIR spectra of the samples of ochre (C₅₋₁₈-a) and blue-green (C₅₋₁₆-b) paints that highlight the use of golden ochre (465 and 407 cm^{-1}) (a) and hydrated Chromium green oxide ($632, 538, 523, 459,$ and 435 cm^{-1}) (b), respectively.

Using ATR-FTIR, it was also possible to distinguish a relatively intense band at ca. 1539 cm^{-1} (in C1, C3, C5, and C7). This might correspond with the $\nu_a \text{ COO}^-$ band, which is associated with metal soaps occurring from the saponification reaction mostly reported as a consequence of the interaction between lead white (basic lead carbonate, $2\text{PbCO}_3 \times \text{Pb(OH)}_2$) and/or zinc white (zinc oxide, ZnO) with the oil binder or oil/egg-based temperas [61–63]. Saponification occurring in paint layers of artworks represents a serious degradation process affecting the appearance and stability of paintings [64]. Thus, its effects might be the appearance of protrusions as well as an increase in the transparency of the paint, brittleness, efflorescence, paint losses, delamination, and even cracks [65]. In the case of Cadorin, the metal soaps were most probably zinc stearates/palmitates as he seems to have employed zinc white not only for rendering the white paint, but also as an extender.

GC-MS allowed the identification of the organic components that were present in the samples. Table 1 indicates the short and long-chain saturated monocarboxylic acids (lauric, myristic, palmitic, and stearic acids), the saturated dicarboxylic fatty acids (azelaic, suberic, and sebacic acids), traces of unsaturated fatty acids (such as oleic acid), and glycerol that were detectable in all the registered chromatograms. All these compounds are clearly visible in the chromatogram of C₇₋₂₂ (shown in Appendix B, Figure A3).

The literature on drying oils mentions that a confirmative value for their presence could be the percentage of total dicarboxylic acids (ΣD , as the sum of azelaic, suberic, and sebacic acids) above 40% and the ratio of azelaic acid to palmitic acid (A/P) above 1.0 [66]. In the present case, ΣD values respect this condition (in C4, C5, C6, and C7) even if the main assumption is that drying oil is not the only lipid binder (Table 2). Moreover, the A/P ratio proved to be between 0.3 and 1 in all cases except for sample C₇₋₂₂. These values likely suggest

the use of *tempera grassa* [23,25]. It should be mentioned that azelaic acid is the main oxidation product of siccative oil, together with other dicarboxylic acids, such as suberic and sebacic [67]. Still, for identifying the type of siccative oil that has been generally used, the P/S ratio is recommended [68]. In the present study, this ratio was in some cases inefficient as most probably both egg and oil fractions were present [23]. However, the ratio was between 1 and 2 in all paintings, which might still accentuate the use of linseed oil. Moreover, it should be noted that it has also been previously reported that the nature and concentration of the pigment can significantly alter this ratio when in direct contact with the oil. The only pigment that seems to not influence the drying process of an oil paint seems to be zinc white, since it does not take part in the evaporation rate at a molecular level [66]. It has also been previously observed that palmitic acid evaporates four times faster than stearic acid [69]; and thus, the P/S ratio value substantially decreases over time [68]. Consequently, the quantity of palmitic acid should be higher in modern and contemporary paintings compared with older historical paintings as has been the case in Guido Cadorin's artworks judging by the P/S ratio values that in C3 and C4 were greater than 2.

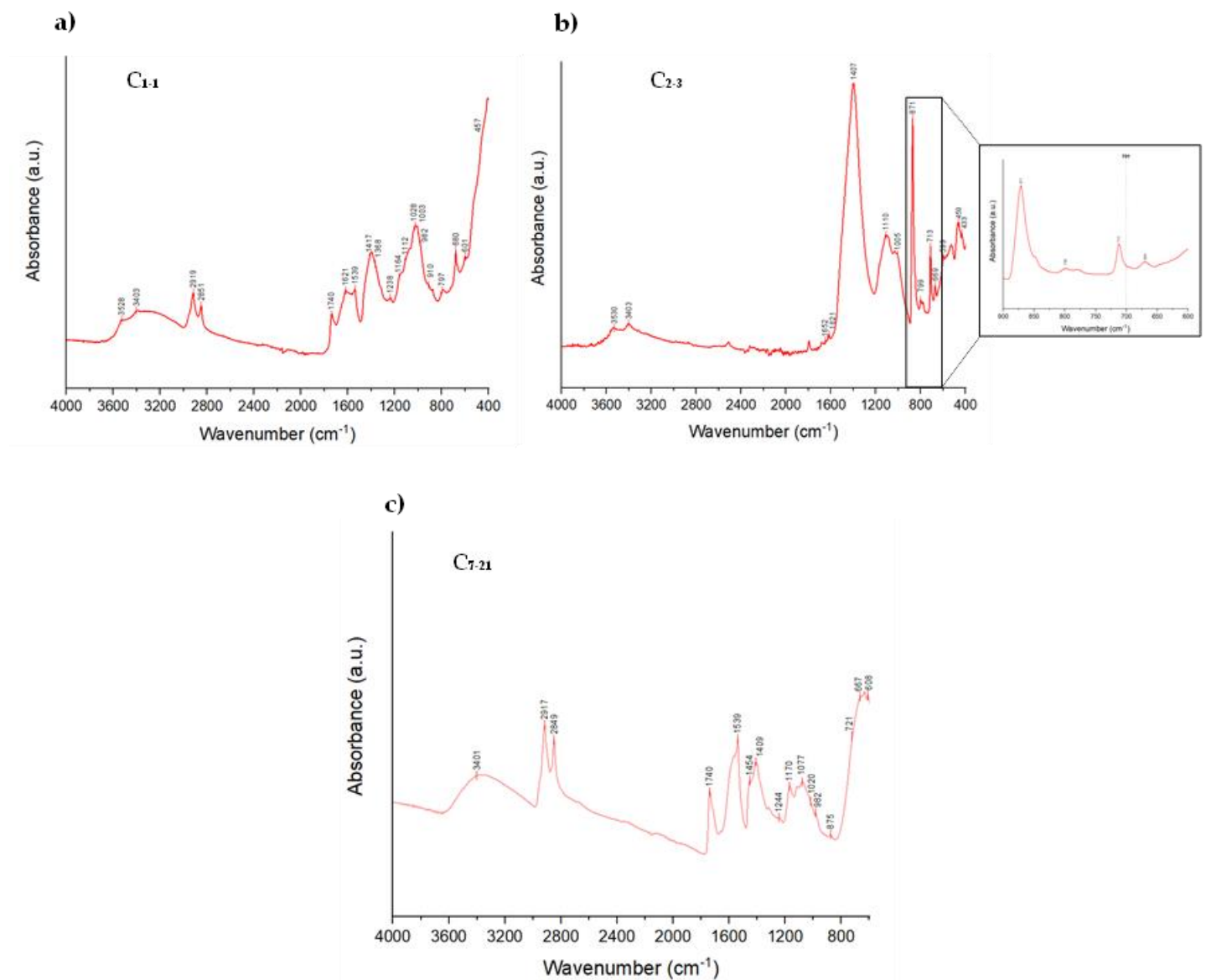


Figure 6. The ATR-FTIR spectra of the samples of red paint (a) C₁₋₁, (b) C₂₋₃, and (c) C₇₋₂₂, which suggest the presence of a lipidic and proteinaceous binder (oil and egg yolk fractions) and metal soaps (namely zinc stearate/palmitate).

Table 1. The retention times and molecular ion masses of the methyl esters that have been attributed to the identified peaks.

N ^o	Retention Time (min)	M ⁺ (g/mol)	Attribution
1	10.79	203.25	Suberic acid dimethyl ester
2	11.76	215.35	Lauric acid methyl ester
3	12.07	217.27	Azelaic acid dimethyl ester
4	13.24	231.30	Sebacic acid dimethyl ester
5	14.09	243.40	Myristic acid methyl ester
6	16.20	271.45	Palmitic acid methyl ester
7	17.89	297.50	Oleic acid methyl ester
8	18.11	299.50	Stearic acid methyl ester
9	19.03	313.53	Nonadecanoic acid methyl ester (Int. Std.)
10	20.00	107.07	Glycerol *
11	20.14	315.46	Dehydroabiestic acid methyl ester
12	21.09	343.50	Tetradehydroabiestic acid, 7-methoxy-methyl ester
13	22.08	329.40	7-Oxodehydroabiestic acid methyl ester
14	23.45	417.60	15-Hydroxy-7-oxodehydroabiestic acid methyl ester

* According to Izzo [25], after passing the electrospray ionization process, glycerol fragmentates into a variety of different derivatives; however, only the most abundant ones are reported in this table.

Table 2. Summary of the GC/MS analyses. Quantitative and qualitative results for fatty acids and other organic compounds.

		Paint Samples																
		C1-1	C1-2	C2-3	C2-4	C2-5	C3-7	C3-9	C3-10	C4-13	C4-14	C5-15	C5-16	C5-18	C6-19	C7-21	C7-22	
Observed Color using OM		White + Black + Red + Blue	Black	Red + Blue	Blue	Black	Black	White	Black + BG	Black	White + Black + Red + Blue	Red	Blue + Green	Yellow	White + Black + Red + Blue	White + Red	Red	
	Observed varnish on OM	x	x	-	-	-	x	?	x	?	x	x	x	x	x	-	-	
Fatty acids and other compounds	Suberic acid dimethyl ester	1.99	2.45	1.43	1.58	-	4.32	5.31	-	-	3.76	2.58	6.64	7.68	5.53	3.82	8.72	
	Lauric acid methyl ester	2.80	2.79	5.28	5.97	6.26	8.40	5.19	7.55	5.14	3.00	1.53	1.02	0.93	2.80	0.64	-	
	Azelaic acid dimethyl ester	15.21	15.58	14.34	15.93	9.85	28.87	40.19	12.75	9.56	25.42	13.50	29.03	26.55	26.44	18.25	27.39	
	Sebacic acid dimethyl ester	0.72	0.82	1.27	1.48	-	-	1.80	-	-	1.22	0.81	2.18	2.17	2.14	1.68	5.67	
	Myristic acid methyl ester	9.40	12.69	23.85	22.13	21.54	24.75	16.67	32.69	18.82	8.38	6.24	4.59	4.47	5.14	1.24	3.92	
	Palmitic acid methyl ester	28.29	30.20	20.11	18.61	16.34	78.74	44.50	17.93	28.37	31.20	31.50	30.79	31.65	30.74	23.95	17.49	
	Oleic acid methyl ester	4.55	9.41	2.50	2.29	1.42	2.40	6.59	1.83	1.34	5.62	3.75	2.45	3.10	4.37	18.78	5.13	
	Stearic acid methyl ester	30.04	17.71	21.22	18.16	33.03	61.59	14.64	19.57	25.27	11.93	31.38	19.43	19.61	15.33	13.48	18.31	
	Glycerol	6.10	7.57	10.00	13.86	11.56	29.14	15.55	10.31	11.48	9.48	6.95	3.21	3.35	6.43	15.40	11.45	
	Dehydroabiestic acid methyl ester	x	x	-	x	-	x	x	-	-	x	x	x	x	x	x	x	x
	Tetradehydroabiestic acid, 7-methoxy-methyl ester	x	-	-	x	-	-	-	-	-	x	x	x	x	x	x	x	x
	7-Oxodehydroabiestic acid methyl ester	-	-	-	x	-	-	-	-	-	x	x	x	x	-	x	x	
	15-Hydroxy-7-oxodehydroabiestic acid methyl ester	-	-	-	-	-	-	-	-	-	-	-	-	-	-	x	x	
Molar ratios among fatty acids	P/S	0.94	1.71	0.95	1.02	0.49	1.28	3.04	0.92	1.12	2.62	1.00	1.58	1.61	2.00	1.78	0.96	
	A/P	0.54	0.52	0.71	0.86	0.60	0.37	0.90	0.71	0.34	0.81	0.43	0.94	0.84	0.86	0.76	1.57	
	D/P	0.63	0.62	0.85	1.02	0.36	0.38	1.60	0.73	2.91	2.27	0.54	1.23	1.15	1.11	1.31	2.39	
	ΣD	17.93	18.84	17.04	18.99	5.84	12.72	47.30	12.80	82.40	70.80	16.90	37.80	36.40	34.11	31.50	41.78	
	O/S	0.15	0.53	0.12	0.13	0.04	0.04	0.45	0.09	0.05	0.47	0.12	0.13	0.16	0.29	1.39	0.28	
	A/Sub	7.63	6.37	10.00	10.05	-	6.69	7.56	-	-	6.77	5.23	4.37	3.46	4.78	4.77	3.14	

Regarding the maturity of the oil, the O/S ratio was generally around 0.1–0.2 in all the analyzed artworks, which emphasizes the oxidation of the double bond within the oleic acid, which usually has a low content in aged paintings [70].

3.4. Varnish Layers, Other Additives and Their Degradation Products

The presence of protective coatings was emphasized through OM, as a thin translucent film was clearly covering the samples collected from five paintings, namely C1, C3, C4, C5, and C6. It is noteworthy that the varnish layers seemed to be characterized by a more pronounced yellowing in the case of the older paintings rendered around 1930 (C1 and C3), which might suggest the predominance of oxidation products. Raman spectroscopy allowed the identification of a peak that might have underlined the use of a diterpenic resin at ca. 3080 cm^{-1} in C1, C4, and C5 [71]. However, the GC-MS analysis confirmed this result through the identification of dehydroabietic acid (DHA)-methyl ester, 7-methoxy-tetra-DHA-methyl ester, 7-oxo-DHA-methyl ester, and 15-hydroxy-7-oxo-DHA-methyl ester, the first compound being detected in all paintings according to Table 2. These four oxidation products derive from the natural aging of the abietic acid [72–75], which is a marker compound of a resinous material, namely a diterpenic resin from the *Pinaceae* family. Thus, these findings highlight the use of pine colophony or Venice turpentine. However, the latter is generally determined by the presence of larixol and larixyl acetate (in high amounts) [73], which have not been identified in this case. It should be noted that the presence of these compounds in the case of C2 and C7 that were not covered by a varnish layer highlights the use of this natural resin as an additional binding medium. Its purpose might have been to alter the rheological properties of paints, according to Giorgio De Chirico [38], an Italian artist contemporary to Guido Cadorin. Moreover, Table 2 highlights that samples generally presented high levels of glycerol content, which as Giorgio De Chirico suggested, improves the “elasticity” of paint [38]. Furthermore, Ortiz Miranda et al. [76] stressed that commercial preprimed canvas during this period usually consisted of one or more preparatory layers containing white pigments and fillers such as lead white, barium white/lithopone, zinc white and calcium carbonate/calcite, which were sometimes mixed with plasticizers and other additives (e.g., non-drying oils, honey, glycerin, sugar, soaps) to extend the shelf-life of paint. Another aspect that is worth noting is that the presence of gum Arabic or other polysaccharidic materials could not be entirely ensured, as the GC-MS method that was used was mainly developed for the identification of fatty acids. Despite this, the strong and representative Raman peak for tree resins (such as gum Arabic and gum tragacanth) was found at ca. 2926 cm^{-1} [30], though this band might be generally attributed to lipid-based binding media since it corresponds to symmetric and asymmetric C-H stretching [77]. Thus, further research should be conducted to enhance the knowledge on the use of these materials by the artist.

3.5. The Technique of Guido Cadorin

Regarding easel paintings, Guido Cadorin seems to have indeed preferred the use of a mixture of siccative oils (mainly linseed oil), natural resins (pine colophony or Venice turpentine), proteins (from both egg yolk and animal glue), and polysaccharides (such as gum Arabic) and glycerol (Table 2). The latter ones might have also had the role of a binding media as they rendered the paint layer easier to apply and form a thin glaze. Regarding fresco paintings as in the case of C2, the artist opted for a casein-based binding medium. Furthermore, the predilection of the artist for the use of traditional self-prepared materials appears to be correct, according to the results provided by Raman spectroscopy. C1, which is dated to 1922–23, and thus is the oldest from the painting collection that was taken into consideration, is characterized by the presence of notoriously used pigments in the history of art, such as red ochre (Fe_2O_3), carbon-black, and ultramarine blue. However, from around 1940, he might have started to implement industrial oil paints, such as titanium white replaced zinc white/calcite/lithopone, which could have been more easily procured. Furthermore, he seemed to have started to use paint tubes since traces of zinc white were also found in the

titanium white paint, which might have acted as an additive. In spite of this, the artist appears to have opted for the use of a compressed color palette at the beginning of his career until 1930 composed of primary and neutral colors, all the rest being obtained through mixtures. This tendency started to change from 1930 on as pure chromophore secondary pigments were introduced such as hydrated chromium green oxide.

4. Conclusions

The multi-analytical approach applied to the study of the seven artworks of Guido Cadorin proved to be efficient in the identification of the painting materials and description of the artist's technique and its evolution through time. Thus, it was further confirmed that Guido Cadorin had a predilection for *tempera grassa*, which was detected in all paintings, an outcome that is in accordance with the previous research [7]. The pigments and inorganic additives could be identified through spectroscopic techniques, namely HSI, Raman, XRF, and ATR-FTIR. Therefore, it could be observed that the artist mainly preferred the use of a compressed color palette, which consisted mainly of black, white, blue, and red. Initially, in the case of C1, C2, and C3 (depicted around 1930), he seems to have employed only carbon-black, zinc white/calcite/lithopone, ultramarine blue, and hematite, but from C4 onwards (depicted after 1940) he started to use titanium white together with zinc white, cinnabar red instead of hematite, whilst he continued to use carbon-black and ultramarine blue. However, he also began to use green and ochre, the former being green chromium oxide and the latter Italian golden ochre. However, further study is recommended on the extracted samples in cross-section using scanning electron microscopy coupled with an energy dispersive microanalytical system (SEM/EDS) [78] to better observe the stratigraphy, obtain the elemental composition of the constituent layers, and identify the presence of mixtures of pigments.

A lipid-based binding medium was observed in all artworks, through the use of Raman and ATR-FTIR, which was assigned to either oil and/or egg yolk, as the latter was previously assumed due to the knowledge of its use in the paintings of Cesare Laurenti, who was the master of Guido Cadorin and whose recipes were closely followed by his apprentice [7]. However, its presence could be attested only by the bands corresponding to Amide I and III, which could have also been attributed to animal glue that could have been present in the ground layers. Despite this, GC-MS gave further insight into the type of oil that was used, which was siccative; and according to the P/S molar ratio, seemed to have been linseed oil in all cases. Still, the presence of egg yolk could not be ensured, as it is well-known that one of the limitations of this technique is the identification of proteinaceous compounds such as ovalbumin in this case [79]. Therefore, further research is recommended to fully emphasize the presence of egg yolk and/or animal glue, which could be made through the enzyme-linked immunosorbent assay (ELISA) procedure [80].

Another important outcome of the application of GC-MS was the detection of the methyl esters of diterpenic resins belonging to the *Pinaceae* family, which are characteristic to either colophony or Venice turpentine, both in the paintings that, according to OM, presented a varnish layer (C1, C3, C4, C5, C6), and in those that did not (C2, C7) highlighting the double role of the material as a varnish and a binding medium. Moreover, it should be noted that pine colophony tends to darken and gradually become brittle, which might enhance the need for the employment of specific conservation measures [74].

Therefore, it is highly likely that Guido Cadorin prepared his paints himself before and around 1930 as he added multiple binding media to the pigments to obtain the desired consistency of his *tempera grassa*. However, this tendency seemed to change from 1940 on since it is highly likely that titanium white was applied from a paint tube. Moreover, all the employed canvases appear to have been commercially primed, as the presence of barite/lithopone could be observed in all paintings, and since the artist manufactured his own paints, the probability is quite low for its use as a filler. Moreover, lead white was additionally observed, solely when the backside of the canvas of C4 was analyzed. Therefore, it was not detected in the white paint, which was shown to mainly consist of

titanium white in anatase form, which might confirm this assumption. However, the main component of the preparatory layer of the canvas was gypsum, which was detected in all paintings. In other words, the color palette together with the binding media and varnishes of Guido Cadorin could be identified and described through the employed techniques.

Author Contributions: Conceptualization, F.C.I. and E.G.M.T.; methodology, F.C.I., E.G.M.T., T.R. and L.F.; investigation, F.C.I., E.G.M.T., T.R. and L.F.; resources, E.B. and M.P.; data curation, F.C.I., E.G.M.T., T.R. and L.F.; writing—original draft preparation, F.C.I., E.G.M.T. and T.R.; writing—review and editing, F.C.I., E.G.M.T. and T.R.; supervision, F.C.I.; project administration, F.C.I. All authors have read and agreed to the published version of the manuscript.

Funding: This research received no external funding.

Data Availability Statement: Not applicable.

Acknowledgments: This study was made possible thanks to the research agreement between MUVE and the research group of “Heritage and Conservation Science” at the Ca’ Foscari University of Venice. The authors want to thank G. Belli and P. Genovesi from MUVE for the fruitful collaboration. The authors would also like to thank the Patto per lo Sviluppo della Città di Venezia (Comune di Venezia) for the support in the research. Teresa Perusini and the artist Giovanni Soccol are fully acknowledged for their suggestions on Cadorin’s techniques.

Conflicts of Interest: The authors declare no conflict of interest.

Appendix A

Table A1. The sampling points and collected micro-samples observed using OM.




Painting Index	Sampling Points	Micro-Samples Observed Using OM	
C1		 <p data-bbox="1265 742 1400 798"><i>Sample 1</i> Objective: 1.5x</p> <p data-bbox="1323 847 1386 882">C1-1</p>	 <p data-bbox="1675 742 1809 798"><i>Sample 2</i> Objective: 1.5x</p> <p data-bbox="1727 847 1789 882">C1-2</p>

Table A1. Cont.



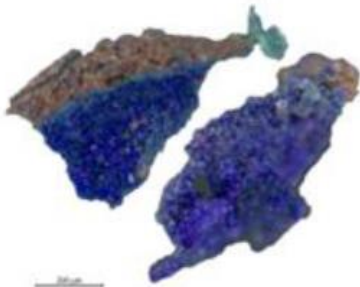

Painting Index	Sampling Points	Micro-Samples Observed Using OM		
C2				
		<i>Sample 3</i> <i>Objective: 0.63x</i>	<i>Sample 4</i> <i>Objective: 1.5x</i>	<i>Sample 5</i> <i>Objective: 1.5x</i>
		C2-3	C2-4	C2-5

Table A1. Cont.

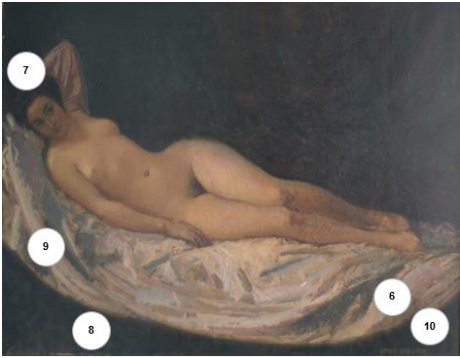
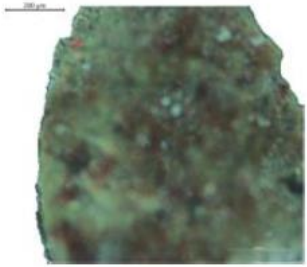
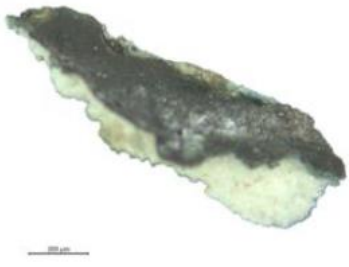

Painting Index	Sampling Points	Micro-Samples Observed Using OM		
C3				
		<p><i>Sample 6</i> <i>Objective: 0.63x</i></p>	<p><i>Sample 7</i> <i>Objective: 1.5x</i></p>	<p><i>Sample 8</i> <i>Objective: 1.5x</i></p>
		C ₃₋₆	C ₃₋₇	C ₃₋₈

Table A1. Cont.

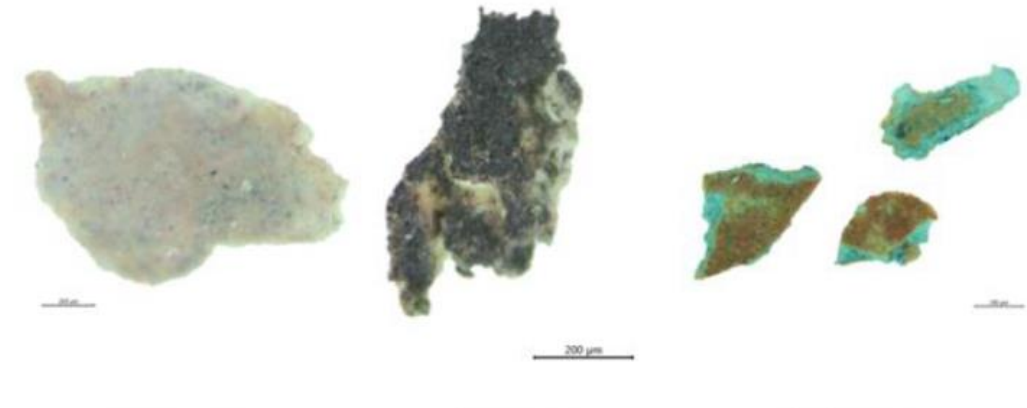
Painting Index	Sampling Points	Micro-Samples Observed Using OM
C4		 <p data-bbox="1055 767 2078 858"><i>Sample 12</i> <i>Objective: 0.63x</i></p> <p data-bbox="1435 767 1659 858"><i>Sample 13</i> <i>Objective: 1.5x</i></p> <p data-bbox="1809 767 2078 858"><i>Sample 14</i> <i>Objective: 1.5x</i></p>
		<p data-bbox="1200 943 1290 983">C4-12</p> <p data-bbox="1514 943 1603 983">C4-13</p> <p data-bbox="1850 943 1939 983">C4-14</p>

Table A1. Cont.

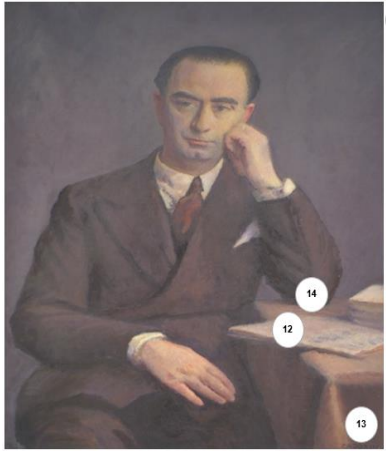
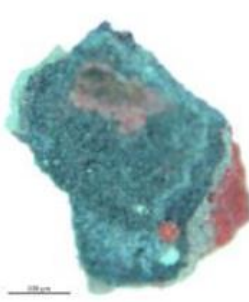








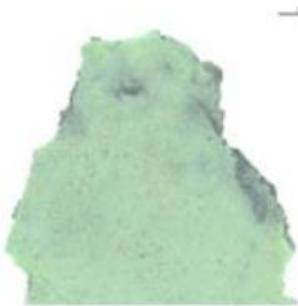

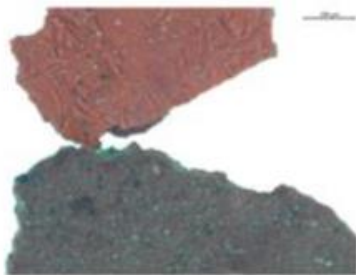
Painting Index	Sampling Points	Micro-Samples Observed Using OM			
<p>C5</p> 					
		<p>Sample 15 Objective: 0.63x</p>	<p>Sample 15-behind Objective: 1.5x</p>	<p>Sample 16 Objective: 1.5x</p>	
		<p>C5-15</p>	<p>C5-15b</p>	<p>C5-16</p>	
					
			<p>Sample 16-behind Objective: 1.5x</p>	<p>Sample 17 Objective: 1.5x</p>	<p>Sample 18 Objective: 1.5x</p>
			<p>C5-16b</p>	<p>C5-17</p>	<p>C5-18</p>

Table A1. Cont.

Painting Index	Sampling Points	Micro-Samples Observed Using OM
C6		 <p data-bbox="1467 810 1668 901"><i>Sample 19</i> <i>Objective: 1.5x</i></p>

C₆₋₁₉

Table A1. Cont.

Painting Index	Sampling Points	Micro-Samples Observed Using OM		
C7				
		Sample 20 Objective: 1.5x	Sample 21 Objective: 1.5x	Sample 22 Objective: 1.5x
		C7-20	C7-21	C7-22

Appendix B

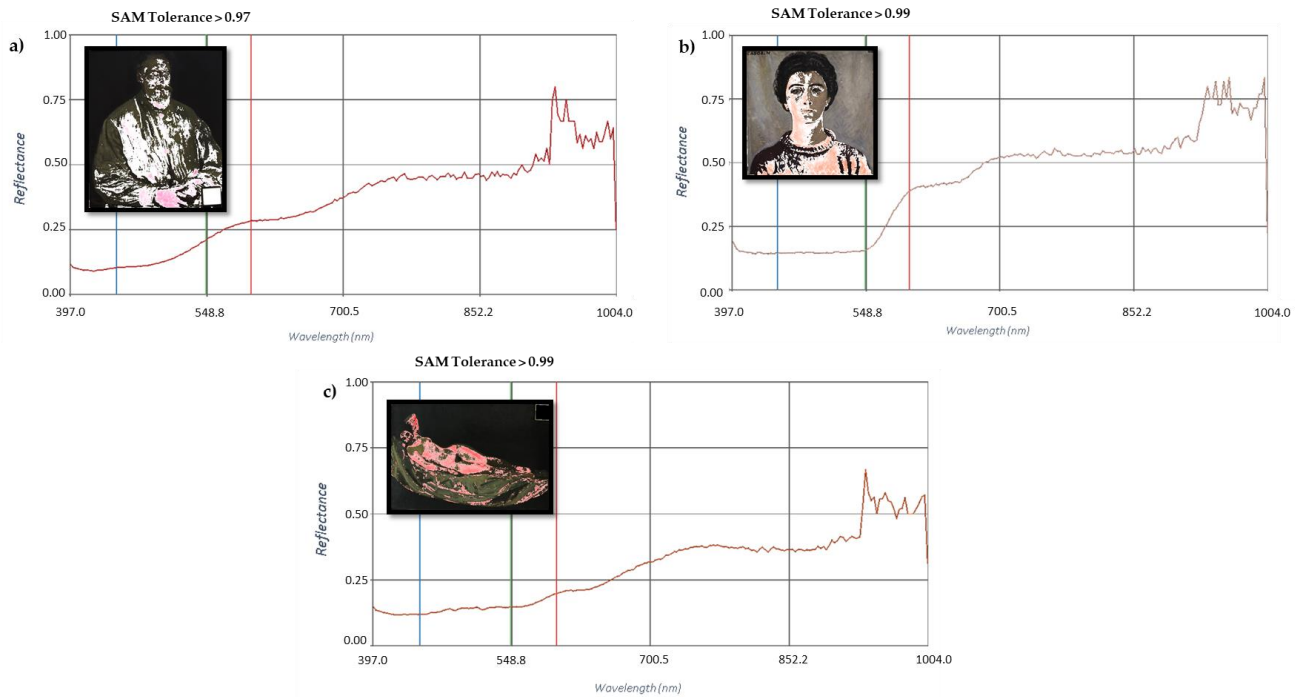


Figure A1. The HSI reflectance spectra of the red paint in C1 (a), C2 (b), and C3 (c) that highlight the use of hematite. The corresponding maps of the identified red pigments are also included together with the SAM tolerance values.

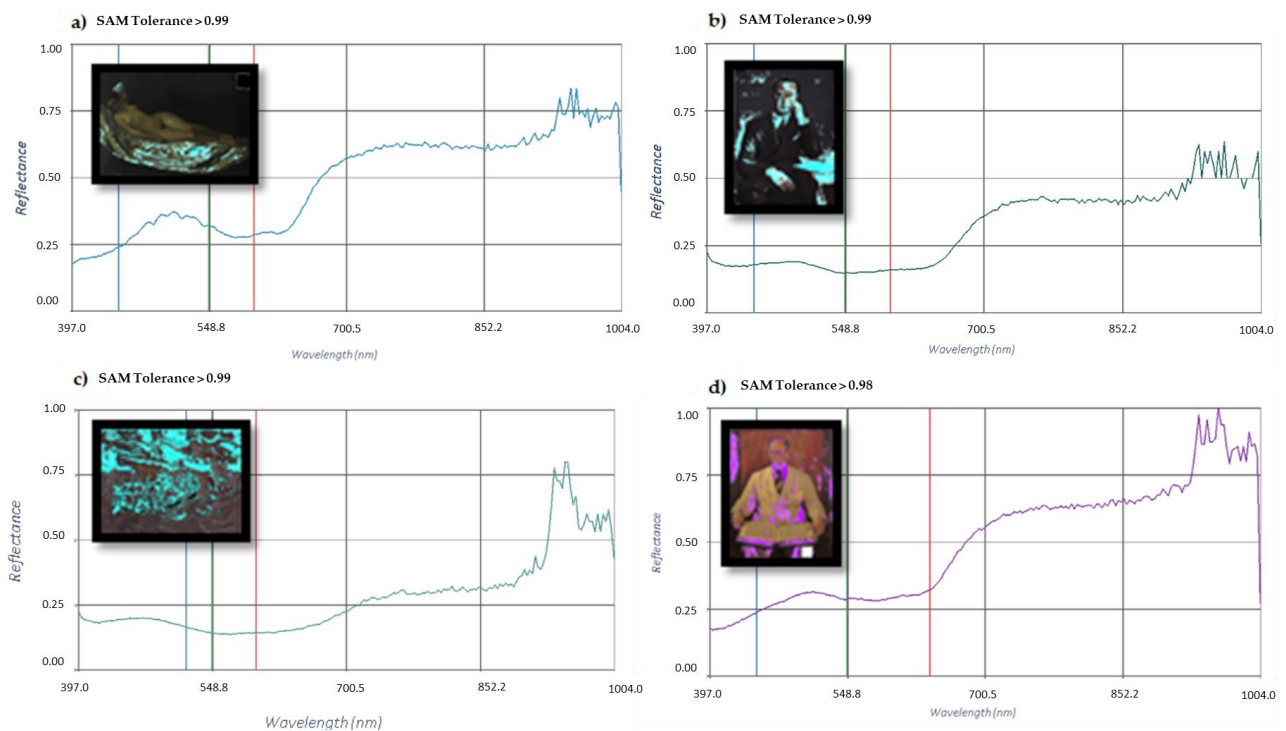


Figure A2. The reflectance spectra of the blue paint in C3 (a), C4 (b), C5 (c) and C6 (d) that highlight the use of ultramarine blue. The corresponding maps of the identified red pigments are also included together with the SAM tolerance values.

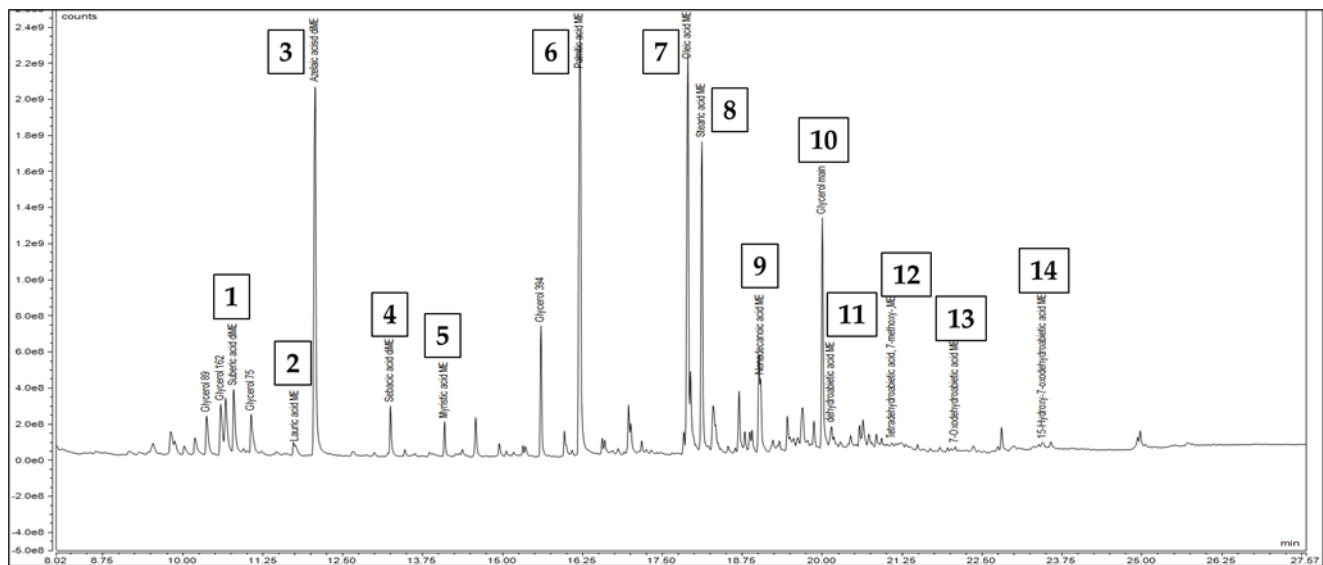


Figure A3. Total Ion Current (TIC) chromatogram after derivatization and analysis of sample C7-22 through GC-MS. Peaks are numbered in accordance with the attributions shown in Table 1.

References

- Beltinger, K. The Tempera Revival 1800–1950: Historical Background, Methods of Investigation and the Question of Relevance. In *Tempera Painting 1800–1950: Experiment and Innovation from the Nazarene Movement to Abstract Art*; Archetype Publications Ltd.: London, UK, 2019; pp. 13–20.
- Perusini, G.; Perusini, T. The use of tempera by painters and restores in Italy and Latin Europe, c. 1800–1870. In *Painting in Tempera, c. 1900*; Swiss Institute for Art Research: London, UK, 2016; pp. 25–38.
- Perusini, T.; Perusini, G.; Izzo, F.C.; Soccol, G. Tempera Painting in Veneto at the Beginning of the 20th Century. In *Tempera Painting 1800–1950. Experiment and Innovation from the Nazarene Movement to Abstract Art*; Archetype Publications Ltd.: London, UK, 2019; pp. 97–106.
- Dal Canton, G. *Guido Cadorin 1892-1976*; Marsilio: Venice, Italy, 2007.
- Rinaldi, S. Le Tempere Veneziane Di Mariano Fortuny. In *L'Immagine tra Materiale e Virtuali. Contributi in Onore di Silvia Bordini*; Academia: San Francisco, CA, USA, 2013.
- Izzo, F.C.; Zanin, C.; Keulen, H.; Roit, C. From Pigments to Paints: Studying Original Materials from the Atelier of the Artist Mariano Fortuny y Madrazo. *Int. J. Conserv. Sci.* **2017**, *8*, 547–564.
- Izzo, F.C.; Perusini, G. Le Tempere Di De Maria, Laurenti, Cadorin, Favai e Casorati: Riscontri Tra Documenti d'archivio, Prove Di Ricostruzione e Analisi Scientifiche. In *Tecnica Della Pittura in Italia Fra Ottocento e Novecento, Atti Del Convegno, Venezia 23/03/19*; Sargon: Padova, Italy, 2021; pp. 125–149.
- Behmann, J.; Acebron, K.; Emin, D.; Bennertz, S.; Matsubara, S.; Thomas, S.; Bohnenkamp, D.; Kuska, M.T.; Jussila, J.; Salo, H.; et al. Specim IQ: Evaluation of a New, Miniaturized Handheld Hyperspectral Camera and Its Application for Plant Phenotyping and Disease Detection. *Sensors* **2018**, *18*, 441. [[CrossRef](#)] [[PubMed](#)]
- Cucci, C.; Casini, A.; Stefani, L.; Piccolo, M.; Jussila, J. Bridging Research with Innovative Products: A Compact Hyperspectral Camera for Investigating Artworks: A Feasibility Study. In *Proceedings of the Optics for Arts, Architecture, and Archaeology VI*, Munich, Germany, 25–29 June 2017; Volume 10331, pp. 17–29.
- Hayem-Ghez, A.; Ravaud, E.; Boust, C.; Bastian, G.; Menu, M.; Brodie-Linder, N. Characterizing Pigments with Hyperspectral Imaging Variable False-Color Composites. *Appl. Phys. A* **2015**, *121*, 939–947. [[CrossRef](#)]
- Rashmi, S.; Addamani, S.; Ravikiran, A. Spectral Angle Mapper Algorithm for Remote Sensing Image Classification. *Int. J. Innov. Sci. Eng. Technol.* **2014**, *50*, 201–205.
- Marcello Piccolo, A.C. A New Compact VNIR Hyperspectral Imaging System for Non-Invasive Analysis in the FineArt and Architecture Fields. Available online: <https://books.fupress.com/catalogue/a-new-compact-vnir-hyperspectral-imaging-system-for-non-invasive-analysis-in-the-fineart-and-archite/4227> (accessed on 15 December 2022).
- Piccolo, M.; Cucci, C.; Casini, A.; Stefani, L. Hyper-Spectral Imaging Technique in the Cultural Heritage Field: New Possible Scenarios. *Sensors* **2020**, *20*, 2843. [[CrossRef](#)]
- Košek, F.; Culka, A.; Rousaki, A.; Vandenabeele, P.; Jehlička, J. Evaluation of Handheld and Portable Raman Spectrometers with Different Laser Excitation Wavelengths for the Detection and Characterization of Organic Minerals. *Spectrochim. Acta Part A Mol. Biomol. Spectrosc.* **2020**, *243*, 118818. [[CrossRef](#)]
- Odelli, E.; Rousaki, A.; Raneri, S.; Vandenabeele, P. Advantages and Pitfalls of the Use of Mobile Raman and XRF Systems Applied on Cultural Heritage Objects in Tuscany (Italy). *Eur. Phys. J. Plus* **2021**, *136*, 449. [[CrossRef](#)]

16. Culka, A.; Hyršl, J.; Jehlička, J. Gem and Mineral Identification Using GL Gem Raman and Comparison with Other Portable Instruments. *Appl. Phys. A* **2016**, *122*, 959. [CrossRef]
17. NIST. X-ray Transition Energies Database. 2009. Available online: <https://www.nist.gov/pml/x-ray-transition-energies-database> (accessed on 14 December 2022).
18. Deslattes, R.D.; Kessler, E.G.; Indelicato, P.; de Billy, L.; Lindroth, E.; Anton, J. X-ray Transition Energies: New Approach to a Comprehensive Evaluation. *Rev. Mod. Phys.* **2003**, *75*, 35–99. [CrossRef]
19. Carava, S.; Roldan Garcia, C.; Vazquez de Agredos-Pascual, M.L.; Murcia Mascaros, S.; Izzo, F.C. Investigation of modern oil paints through a physico-chemical integrated approach. Emblematic cases from Valencia, Spain. *Spectrochim. Acta Part A Mol. Biomol. Spectrosc.* **2020**, *240*, 118633. [CrossRef]
20. Fuster-López, L.; Izzo, F.C.; Damato, V.; Yusà-Marco, D.J.; Zendri, E. An insight into the mechanical properties of selected commercial oil and alkyd paint films containing cobalt blue. *J. Cult. Herit.* **2019**, *35*, 225–234. [CrossRef]
21. Izzo, F.C.; van den Berg, K.J.; van Keulen, H.; Ferriani, B.; Zendri, E. Modern Oil Paints—Formulations, Organic Additives and Degradation: Some Case Studies. In *Issues in Contemporary Oil Paint*; van den Berg, K.J., Burnstock, A., de Keijzer, M., Krueger, J., Learner, T., de Tagle, A., Heydenreich, G., Eds.; Springer International Publishing: Cham, Switzerland, 2014; pp. 75–104.
22. Bonaduce, I.; Andreotti, A. Py-GC/MS of Organic Paint Binders. In *Organic Mass Spectrometry in Art and Archaeology*; Wiley: New York, NY, USA, 2009; pp. 303–326.
23. Fuster-López, L.; Izzo, F.C.; Andersen, C.K.; Murray, A.; Vila, A.; Picollo, M.; Stefani, L.; Jiménez, R. Picasso's 1917 paint materials and their influence on the condition of four paintings. *SN Appl. Sci.* **2020**, *2*, 2159. [CrossRef]
24. Schilling, M.; Khanjian, H.; Carson, D.M. Fatty Acid and Glycerol Content of Lipids; Effects of Ageing and Solvent Extraction on the Composition of Oil Paints = Acides Gras et Glycerol Des Lipides; Effets Du Vieillissement Sur La Composition Des Peintures a l'huile et Extraction Par Solvant. *Technique La Sci. Au Serv. De L'histoire De L'art Et Des Civilis.* **1997**, *5*, 71–78.
25. Izzo, F.C.; Källbom, A.; Nevin, A. Multi-Analytical Assessment of Bodied Drying Oil Varnishes and Their Use as Binders in Armour Paints. *Heritage* **2021**, *4*, 3402–3420. [CrossRef]
26. Marucci, G.; Beeby, A.; Parker, A.W.; Nicholson, C.E. Raman Spectroscopic Library of Medieval Pigments Collected with Five Different Wavelengths for Investigation of Illuminated Manuscripts. *Anal. Methods* **2018**, *10*, 1219–1236. [CrossRef]
27. Murphy, J. CHAPTER 7—Modifying Specific Properties: Appearance—Black and White Pigmentation. In *Additives for Plastics Handbook*, 2nd ed.; Murphy, J., Ed.; Elsevier Science: Amsterdam, The Netherlands, 2001; pp. 73–92. ISBN 978-1-85617-370-4.
28. Rogge, C.; Arslanoglu, J. Luminescence of Coprecipitated Titanium White Pigments: Implications for Dating Modern Art. *Sci. Adv.* **2019**, *5*, eaav0679. [CrossRef]
29. Gunasekaran, S.; Anbalagan, G.; Pandi, S. Raman and Infrared Spectra of Carbonates of Calcite Structure. *J. Raman Spectrosc.* **2006**, *37*, 892–899. [CrossRef]
30. Burgio, L.; Clark, R.J.H. Library of FT-Raman Spectra of Pigments, Minerals, Pigment Media and Varnishes, and Supplement to Existing Library of Raman Spectra of Pigments with Visible Excitation. *Spectrochim. Acta Part A Mol. Biomol. Spectrosc.* **2001**, *57*, 1491–1521. [CrossRef]
31. Hibberts, S.; Edwards, H.G.M.; Abdel-Ghani, M.; Vandenabeele, P. Raman Spectroscopic Analysis of a 'Noli Me Tangere' Painting. *Philos. Trans. R. Soc. Lond. Ser. A Math. Phys. Eng. Sci.* **2016**, *374*, 20160044. [CrossRef]
32. Lončar, E.S.; Lomić, G.A.; Malbaša, R.V.; Kolarov, L.A. Preparation and Characterization of Aluminum Stearate. *Acta Period. Technol.* **2003**, *34*, 55–60. [CrossRef]
33. Baij, L.; Hermans, J.J.; Keune, K.; Iedema, P. Time-Dependent ATR-FTIR Spectroscopic Studies on Fatty Acid Diffusion and the Formation of Metal Soaps in Oil Paint Model Systems. *Angew. Chem. Int. Ed.* **2018**, *57*, 7351–7354. [CrossRef]
34. van Driel, B.; Phenix, A.; Soldano, A.; Van den Berg, K.J. The Might of White: Formulations of Titanium-Dioxide Based Oil Paints as Evidenced in Archives of Two Artists' Colourmen Mid-Twentieth Century. In Proceedings of the ICOM-CC Triennial Conference Proceedings, Copenhagen, Denmark, 4–8 September 2017.
35. van Driel, B.A.; van den Berg, K.J.; Smout, M.; Dekker, N.; Kooyman, P.J.; Dik, J. Investigating the Effect of Artists' Paint Formulation on Degradation Rates of TiO₂-Based Oil Paints. *Herit. Sci.* **2018**, *6*, 21. [CrossRef]
36. Youssry, M.; Kamand, F.; Magzoub, M.; Nasser, M. Aqueous Dispersions of Carbon Black and Its Hybrid with Carbon Nanofibers. *RSC Adv.* **2018**, *8*, 32119–32131. [CrossRef] [PubMed]
37. Ivory Black—Database of ATR-FT-IR Spectra of Various Materials. Available online: <https://spectra.chem.ut.ee/paint/pigments/ivory-black/> (accessed on 18 November 2022).
38. De Chirico, G. *Piccolo Trattato di Tecnica Pittorica*; Libri Scheiwiller: Milan, Italy, 2001.
39. Aceto, M.; Agostino, A.; Fenoglio, G.; Idone, A.; Gulmini, M.; Picollo, M.; Ricciardi, P.; Delaney, J.K. Characterisation of Colourants on Illuminated Manuscripts by Portable Fibre Optic UV-Visible-NIR Reflectance Spectrophotometry. *Anal. Methods* **2014**, *6*, 1488. [CrossRef]
40. Jubb, A.M.; Allen, H.C. Vibrational Spectroscopic Characterization of Hematite, Maghemite, and Magnetite Thin Films Produced by Vapor Deposition. *ACS Appl. Mater. Interfaces* **2010**, *2*, 2804–2812. [CrossRef]
41. de Faria, D.L.A.; Lopes, F.N. Heated Goethite and Natural Hematite: Can Raman Spectroscopy Be Used to Differentiate Them? *Vib. Spectrosc.* **2007**, *45*, 117–121. [CrossRef]
42. Miguel, C.; Barrocas-Dias, C.; Ferreira, T.; Candeias, A. The Comparative Study of Four Portuguese Sixteenth-Century Illuminated Manueline Charters Based on Spectroscopy and Chemometrics Analysis. *Appl. Phys. A* **2016**, *123*, 72. [CrossRef]

43. Rodríguez-Simón, L.R.; Sol López, V.D.; Ángel LeónColoma, M. Microscopic Identification of Vine Black Pigment in A Tempera Painting By Francisco De Goya. *SM Anal. Bioanal. Tech.* **2017**, *2*, 1–8. [CrossRef]
44. Zumbühl, S.; Zindel, C. *Historical Siccatives for Oil Paint and Varnishes—The Use of Lead Oxide, Alum, White Vitriol, Pumice, Bone Ash and Venetian Glass as Driers: Historical Written Sources—Production and Raw Material Quality—Technological Significance*; HDW Publications: Bern, Switzerland, 2022.
45. *Impiego Della Biacca Nella Pittura*, Legge 19 Luglio 1961, n. 706. Normativa Nazionale Settore: Rome, Italy, 1961; Volume 4.10.
46. Tumosa, C.S.; Mecklenburg, M.F. The Influence of Lead Ions on the Drying of Oils. *Stud. Conserv.* **2005**, *50*, 39–47. [CrossRef]
47. Aceto, M.; Agostino, A.; Fenoglio, G.; Marcello, P. Non-Invasive Differentiation between Natural and Synthetic Ultramarine Blue Pigments by Means of 250–900 Nm FORS Analysis. *Anal. Methods* **2013**, *5*, 4184. [CrossRef]
48. Yivlialin, R.; Galli, A.; Raimondo, L.; Martini, M.; Sassella, A. Detecting the NIR Fingerprint of Colors: The Characteristic Response of Modern Blue Pigments. *Heritage* **2019**, *2*, 2255–2261. [CrossRef]
49. Ultramarine Blue—Database of ATR-FT-IR Spectra of Various Materials. Available online: <https://spectra.chem.ut.ee/paint/pigments/ultramarine-blue/> (accessed on 18 November 2022).
50. Miliani, C.; Rosi, F.; Daveri, A.; Brunetti, B.G. Reflection Infrared Spectroscopy for the Non-Invasive in Situ Study of Artists' Pigments. *Appl. Phys. A* **2011**, *106*, 295. [CrossRef]
51. Montagner, C.; Sanches, D.; Pedroso, J.; Melo, M.J.; Vilarigues, M. Ochres and Earths: Matrix and Chromophores Characterization of 19th and 20th Century Artist Materials. *Acta Part A Mol. Biomol. Spectrosc.* **2013**, *103*, 409–416. [CrossRef]
52. Vahur, S.; Teearu, A.; Leito, I. ATR-FT-IR Spectroscopy in the Region of 550–230 cm⁻¹ for Identification of Inorganic Pigments. *Spectrochim. Acta Part A Mol. Biomol. Spectrosc.* **2010**, *75*, 1061–1072. [CrossRef]
53. Weckhuysen, B.M.; Wachs, I.E. Raman Spectroscopy of Supported Chromium Oxide Catalysts. Determination of Chromium—Oxygen Bond Distances and Bond Orders. *J. Chem. Soc. Faraday Trans.* **1996**, *92*, 1969–1973. [CrossRef]
54. Kendix, E.L. Transmission and Reflection (ATR)Far-Infrared Spectroscopy Applied in the Analysis of Cultural Heritage Materials. Ph.D. Thesis, Alma Mater Studiorum—Università di Bologna, Bologna, Italy, 2009.
55. Pagnin, L. Characterization and Quantification of Modern Painting Materials by IR and Raman Spectroscopies. Master's Thesis, Ca' Foscari University, Venice, Italy, 2017.
56. Hayes, P.A.; Vahur, S.; Leito, I. ATR-FTIR Spectroscopy and Quantitative Multivariate Analysis of Paints and Coating Materials. *Spectrochim. Acta Part A Mol. Biomol. Spectrosc.* **2014**, *133*, 207–213. [CrossRef]
57. Nickless, E.; Holroyd, S. Raman Imaging of Protein in a Model Cheese System. *J. Spectr. Imaging* **2020**, *9*, a9. [CrossRef]
58. Calcite—Database of ATR-FT-IR Spectra of Various Materials. Available online: <https://spectra.chem.ut.ee/paint/fillers/calcite/> (accessed on 19 November 2022).
59. Degioanni, S.; Jurdyc, A.M.; Cheap, A.; Champagnon, B.; Bessueille, F.; Coulm, J.; Bois, L.; Vouagner, D. Surface-Enhanced Raman Scattering of Amorphous Silica Gel Adsorbed on Gold Substrates for Optical Fiber Sensors. *J. Appl. Phys.* **2015**, *118*, 153103. [CrossRef]
60. Rampazzi, L.; Corti, C.; Geminiani, L.; Recchia, S. Unexpected Findings in 16th Century Wall Paintings: Identification of Aragonite and Unusual Pigments. *Heritage* **2021**, *4*, 2431–2448. [CrossRef]
61. Carlyle, L. *The Artist's Assistant: Oil Painting Instruction Manuals and Handbooks in Britain 1800–1900, with Reference to Selected Eighteenth-Century Sources; Oil Painting Instruction Manuals and Handbooks in Britain 1800–1900*; Archetype Publications: London, UK, 2001.
62. Hermans, J.J.; Keune, K.; van Loon, A.; Iedema, P.D. An Infrared Spectroscopic Study of the Nature of Zinc Carboxylates in Oil Paintings. *J. Anal. Atomic Spectrom.* **2015**, *30*, 1600–1608. [CrossRef]
63. Ebert, B.; Osmond, G. Zinc Oxide-Centred Deterioration in 20 Th Century Vietnamese Paintings by Nguyễn Trọng Kiệm (1933–1991). *AICCM Bull.* **2014**, *34*, 4–14. [CrossRef]
64. Švarcová, S.; Kočí, E.; Plocek, J.; Zhankina, A.; Hradilová, J.; Bezdička, P. Saponification in Egg Yolk-Based Tempera Paintings with Lead-Tin Yellow Type I. *J. Cult. Herit.* **2019**, *38*, 8–19. [CrossRef]
65. Izzo, F.C.; Kratter, M.; Nevin, A.; Zendri, E. A Critical Review on the Analysis of Metal Soaps in Oil Paintings. *ChemistryOpen* **2021**, *10*, 904–921. [CrossRef] [PubMed]
66. Tammekivi, E.; Vahur, S.; Vilbaste, M.; Leito, I. Quantitative GC–MS Analysis of Artificially Aged Paints with Variable Pigment and Linseed Oil Ratios. *Molecules* **2021**, *26*, 2218. [CrossRef] [PubMed]
67. Plater, M.J.; De Silva, B.; Gelbrich, T.; Hursthouse, M.B.; Higgitt, C.L.; Saunders, D.R. The Characterisation of Lead Fatty Acid Soaps in 'Protrusions' in Aged Traditional Oil Paint. *Polyhedron* **2003**, *22*, 3171–3179. [CrossRef]
68. Bonaduce, I.; Ribechini, E.; Modugno, F.; Colombini, M.P. Analytical Approaches Based on Gas Chromatography Mass Spectrometry (GC/MS) to Study Organic Materials in Artworks and Archaeological Objects. *Top. Curr. Chem.* **2016**, *374*, 6. [CrossRef]
69. Shilling, M.R.; Carson, D.M.; Khanjian, H.P. Evaporation of Fatty Acids and the Formation of Ghost Images by Framed Oil Paintings. Available online: <https://cool.culturalheritage.org/waac/wn/wn21/wn21-1/wn21-106.html> (accessed on 28 November 2022).
70. Colombini, M.; Modugno, F.; Menicagli, E.; Fuoco, R.; Giacomelli, A. GC-MS Characterization of Proteinaceous and Lipid Binders in UV Aged Polychrome Artifacts. *Microchem. J.* **2000**, *67*, 291–300. [CrossRef]
71. Daher, C.; Paris, C.; Le Hô, A.-S.; Bellot-Gurlet, L.; Échard, J.-P. A Joint Use of Raman and Infrared Spectroscopies for the Identification of Natural Organic Media Used in Ancient Varnishes. *J. Raman Spectrosc.* **2010**, *41*, 1494–1499. [CrossRef]
72. Scalarone, D.; Lazzari, M.; Chiantore, O. Ageing Behaviour and Analytical Pyrolysis Characterisation of Diterpenic Resins Used as Art Materials: Manila Copal and Sandarac. *J. Anal. Appl. Pyrolysis* **2003**, *68–69*, 115–136. [CrossRef]

73. Van den Berg, K.J. *Analysis of Diterpenoid Resins and Polymers in Paint Media and Varnishes. With an Atlas of Mass Spectra*; FOM Institute AMOLF: Amsterdam, The Netherlands, 2012.
74. Ciofini, D.; Striova, J.; Camaiti, M.; Siano, S. Photo-Oxidative Kinetics of Solvent and Oil-Based Terpenoid Varnishes. *Polym. Degrad. Stabil.* **2016**, *123*, 47–61. [[CrossRef](#)]
75. Pintus, V.; Baragona, A.J.; Wieland, K.; Schilling, M.; Miklin-Kniefacz, S.; Haisch, C.; Schreiner, M. Comprehensive Multi-Analytical Investigations on the Vietnamese Lacquered Wall-Panel “The Return of the Hunters” by Jean Dunand. *Sci. Rep.* **2019**, *9*, 18837. [[CrossRef](#)]
76. Ortiz Miranda, A.S.; Kronkright, D.; Walton, M. The Influence of Commercial Primed Canvases in the Manifestation of Metal Soaps Protrusions in Georgia O’Keeffe’s Oil Paintings. *Herit. Sci.* **2020**, *8*, 107. [[CrossRef](#)]
77. Socrates, G.; Socrates, G. *Infrared and Raman Characteristic Group Frequencies: Tables and Charts*, 3rd ed.; Wiley: Chichester, UK; New York, NY, USA, 2001; ISBN 978-0-471-85298-8.
78. Macchia, A.; Biribicchi, C.; Rivaroli, L.; Aureli, H.; Cerafogli, E.; Colasanti, I.A.; Carnazza, P.; Demasi, G.; La Russa, M.F. Combined Use of Non-Invasive and Micro-Invasive Analytical Investigations to Understand the State of Conservation and the Causes of Degradation of I Tesori Del Mare (1901) by Plinio Nomellini. *Methods Protoc.* **2022**, *5*, 52. [[CrossRef](#)]
79. Lluveras-Tenorio, A.; Orsini, S.; Pizzimenti, S.; Del Seppia, S.; Colombini, M.P.; Duce, C.; Bonaduce, I. Development of a GC–MS Strategy for the Determination of Cross-Linked Proteins in 20th Century Paint Tubes. *Microchem. J.* **2021**, *170*, 106633. [[CrossRef](#)]
80. Palmieri, M.; Vagnini, M.; Pitzurra, L.; Brunetti, B.G.; Cartechini, L. Identification of Animal Glue and Hen-Egg Yolk in Paintings by Use of Enzyme-Linked Immunosorbent Assay (ELISA). *Anal. Bioanal. Chem.* **2013**, *405*, 6365–6371. [[CrossRef](#)]

Disclaimer/Publisher’s Note: The statements, opinions and data contained in all publications are solely those of the individual author(s) and contributor(s) and not of MDPI and/or the editor(s). MDPI and/or the editor(s) disclaim responsibility for any injury to people or property resulting from any ideas, methods, instructions or products referred to in the content.